

# New York Bight Indicator Report 2021

MOU #AM10560 NYS DEC & SUNY Stony Brook

Report contributors: Laura K. Gruenburg, Janet A. Nye, Lesley Thorne, Brandon Beltz, Tyler Menz, Baoshan Chen, Eleanor Heywood, Julia Stepanuk, Joe Warren, Charles Flagg

Contact Principal Investigator, Janet A. Nye with questions or comments janet.nye@stonybrook.edu

<b>PART 1: INDICATOR ANALYSIS.....</b>	<b>2</b>
1. EXECUTIVE SUMMARY .....	2
2. REPORT STRUCTURE .....	3
3. PHYSICAL AND CHEMICAL INDICATORS.....	3
<i>Seasonal mean sea surface temperature</i> .....	3
<i>Marine heatwave days</i> .....	5
<i>Bottom temperature anomaly</i> .....	6
<i>Mid-Atlantic Cold Pool Volume and Duration.</i> .....	7
<i>Bottom Dissolved Oxygen</i> .....	8
<i>Aragonite Saturation State and pH</i> .....	8
<i>Mean Wind Stress</i> .....	11
<i>Stratification anomaly</i> .....	12
<i>Hudson River Flow</i> .....	13
<i>Salinity</i> .....	14
<i>Global Carbon Dioxide</i> .....	14
<i>Lobster Thermal Habitat</i> .....	15
<i>Location of Surface 20°C Isotherm</i> .....	16
<i>Summary for Physical and Chemical Indicators</i> .....	18
4. MARINE COMMUNITY .....	21
<i>Monthly mean surface chlorophyll</i> .....	21
<i>Calanus finmarchicus abundance</i> .....	22
<i>Copepod size index</i> .....	23
<i>Commercially important invertebrate biomass</i> .....	23
<i>Forage species biomass</i> .....	26
<i>Aggregate Feeding groups</i> .....	26
<i>Northern vs. Southern finfish and macroinvertebrates</i> .....	28
<i>Ratio of Northern to Southern species biomass</i> .....	30
<i>Ratio of benthic to pelagic species</i> .....	31
<i>Fish species richness</i> .....	32
<i>Average trophic level of fish community</i> .....	33
<i>Temperature preference of the fish community</i> .....	34
<i>Summary for Marine Community Indicators</i> .....	36
5. COASTAL COMMUNITIES .....	36
<i>Recreational harvest (total number all species)</i> .....	36
<i>Commercial fishing landings in NY</i> .....	38
<i>Human population of Long Island</i> .....	38
<i>Sea level risk for Long Island Communities</i> .....	39
<i>Summary for Coastal Community Indicators</i> .....	39
6. CONCLUSIONS AND OUTLOOK FOR 2022 .....	42
7. REFERENCES.....	43

<b>PART 2: INDICATOR DEVELOPMENT .....</b>	<b>45</b>
1. PHYSICAL AND CHEMICAL INDICATORS .....	45
<i>Fall transition date</i> .....	45
<i>Cold Pool Volume</i> .....	45
<i>20°C surface isotherm</i> .....	47
<i>Subsurface aragonite saturation state (<math>\Omega_{Ar}</math>), corresponding pH and percent area.....</i>	49
<i>Bottom Dissolved Oxygen</i> .....	51
2. MARINE COMMUNITY.....	52
<i>Humpback whale body condition</i> .....	52
<i>Odontocete Strandings data</i> .....	53
3. COASTAL COMMUNITIES.....	53
<i>Vessel Density and Speed</i> .....	53
4. REFERENCES.....	54

## Part 1: Indicator Analysis

### 1. Executive Summary

Indicators of ocean temperature are increasing in the New York Bight (NYB) in all seasons, in surface waters and bottom waters. Duration of marine heatwaves continue to be higher than normal, but fortunately we have not seen long-lasting marine heatwaves as we did in 2012 and 2017. Our new indicator of the Mid-Atlantic cold pool (CP), cold pool volume in April, July, and October, shows a change in this feature over the last decade. Specifically, that the Cold pool has become extremely small or completely absent during October. Another new indicator of thermal habitat, the 20°C surface isotherm, illustrates a poleward shift of these warm surface waters. Since 2010 this isotherm is rarely found in the NYB during summer and is now only present in the autumn. These findings are consistent with similar indicators found for the broader Mid-Atlantic (NMFS 2021, NMFS in press) and the recent findings that the oceanographic properties of the Northeast Shelf have fundamentally changed. In 2008, a change in the position of the north wall of the Gulf Stream near the Grand Banks blocked cold, less saline water from the Labrador Current from entering the Northeast Shelf (Neto et al. 2021). The effects of this event can be seen one to two years later in the NYB in all of our physical indicators. Whether this change is permanent remains to be seen, but several lines of evidence suggest that changes in Gulf Stream dynamics will continue to warm the Northeast US Shelf and the NYB through dynamics to the north of NYB and via more frequent interactions with Gulf Stream waters and warm core rings closer to the NYB itself (Joyce et al. 2010, Nye et al. 2010, Gangopadhyay et al. 2019).

In addition to these physical changes, our understanding of the ocean chemistry within the NYB has improved. We have developed new indicators for bottom dissolved oxygen, pH and surface and subsurface aragonite, a mineral critical to shell formation in marine bivalves. Although we do not see aragonite saturation states low enough to inhibit shell-formation ( $\Omega_{Ar} < 1$ ), the highest temperatures, lowest dissolved oxygen levels, and lowest aragonite saturation state all occur in fall. The combined effect of these physio-chemical conditions working in

concert may already be reducing survivorship and growth of commercially-important shellfish such as quahogs and surfclams. Lobster habitat does not appear to be limiting at this time within the NYB, but may be limiting in estuaries and the Long Island Sound, which we did not examine.

The human community indicators did not change very much from our previous reports. We continue to see that marine recreational landings have increased in NY, but most fish are released. Risk to sea level rise did not change, but we examined storm surge risk and find that coastal communities Queens and Kings County are some of the most vulnerable to storm surge not just in NY, but in the nation. The population in coastal NY communities, considered all counties in Long Island, has increased dramatically over time, but there has been a slight decline in recent years.

## **2. Report structure**

Part 1 of this report presents all updated indicators for 2021. Several indicators which were proposed or under development in the previous year have been included here: cold pool volume, bottom dissolved oxygen (DO), subsurface pH and aragonite saturation state, seasonal mean wind stress, lobster thermal habitat, location of 20°C isotherm, northern vs. southern species biomass, structure oriented species biomass, fish species richness, average trophic level of fish community, and temperature preference of fish community. The appendix to this report discusses indicator development including the development of the cold pool indicators, carbonate chemistry indicators, location of the 20°C isotherm, humpback whale body condition, vessel density and speed, and odontocete strandings data.

## **3. Physical and Chemical Indicators**

### *Seasonal mean sea surface temperature*

As noted in the previous report (Indicators Report 2020 Part 2) sea surface temperatures have been increasing since the 1980s across all four seasons within the NYB (Fig. 1). The warming has been greatest in the summer and autumn. Here we define winter as an average of January February, March; spring as April, May, June; summer as July, August, September; and autumn as October, November, December. Changes in seasonal SST are also lengthening the summer season (Fig. 2), where the transition from the warmest temperatures of summer and fall turn to cooler winter temperatures later in the year.

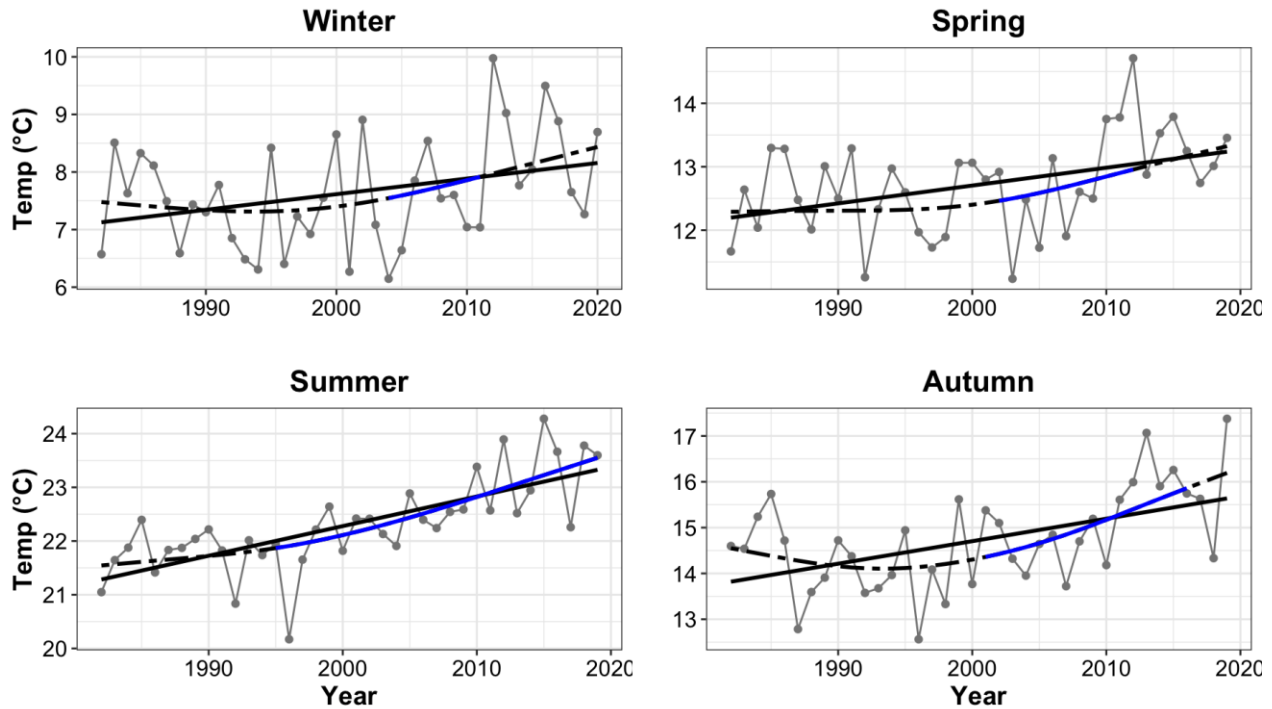


**Figure 1. Seasonal mean sea surface temperature.** Thin solid lines show yearly mean values for each season. A thick black solid line indicates a statistically significant linear trend ( $p < 0.05$ ). The warming trend is the highest during summer. Nonlinear trends of seasonal mean sea surface temperature are shown by the dashed black lines. Solid blue lines indicate a significant increasing trend. The dashed black line indicates no statistically significant trend ( $p < 0.05$ ).

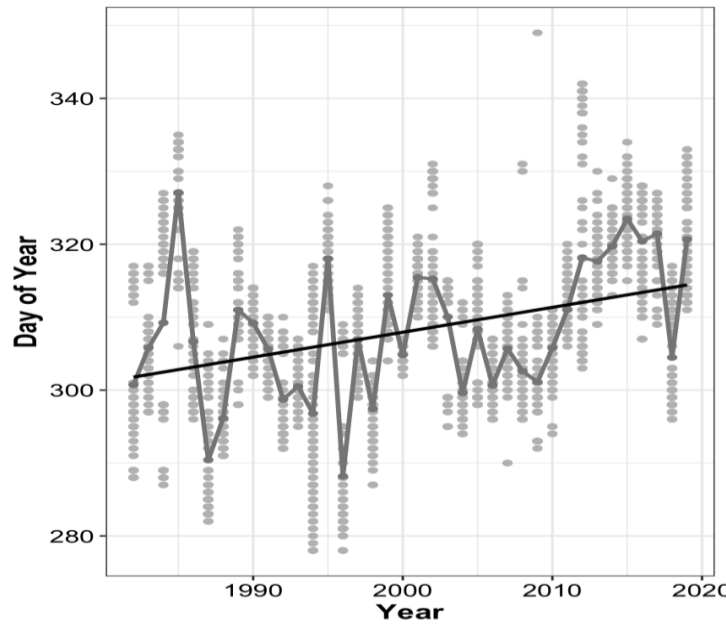


**Figure 2. Seasonal thermal transition in fall.** Looking at sea surface temperature in terms of seasonal transition dates also reveals a warming trend. Over the course of the satellite observational period the day of transition from warmer summer/fall temperatures to cool winter temperatures has gotten later.

### **Marine heatwave days**

As discussed in the 2020 Indicator Report, marine heatwaves have increased in the NYB in the most recent decade and there is a possibility that we have entered a new regime in surface temperature. Although this region has not recently experienced very large heatwaves like the ones in 2012 and 2017, within the last few years we have seen 50-100 days that are hotter than the 95th percentile temperatures seen in the historical record (Fig. 3).

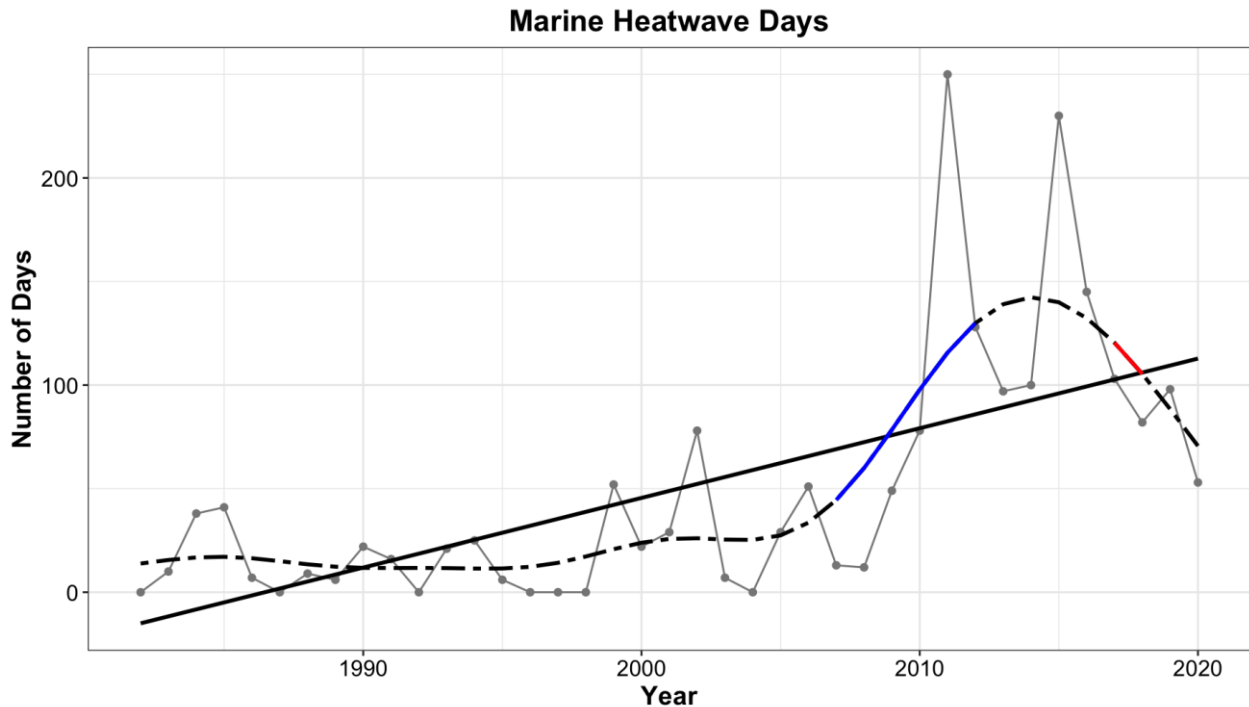


**Figure 3. Number of marine heatwave days per year.** Yearly data is shown by the grey line, the linear trend by the solid black line and the nonlinear GAM by the dashed black line. Periods of statistically significant increasing trend of the GAM are shown in blue and significant decreasing trend in red.

### **Bottom temperature anomaly**

Much like marine heatwaves and seasonal mean SST, annual bottom temperature anomalies are also increasing (Fig. 4). Additional data has been added to bottom temperature anomaly allowing us to extend the time series back to 1941. In the last report the time series extended only back to 1968 using data from XBT, CTD, and Seawolf cruises. Here we also included data from glider and MBT data from the world ocean database. Interestingly, the bottom temperature anomaly is correlated with the AMO index which describes the state of the Atlantic Multidecadal Oscillation with  $r=0.4$  ( $p<0.05$ ). Although the AMO index is calculated using sea surface temperatures, it also shows warmer temperatures during the 1940s, a decrease until the 1970s followed by an increase through the 2010s.

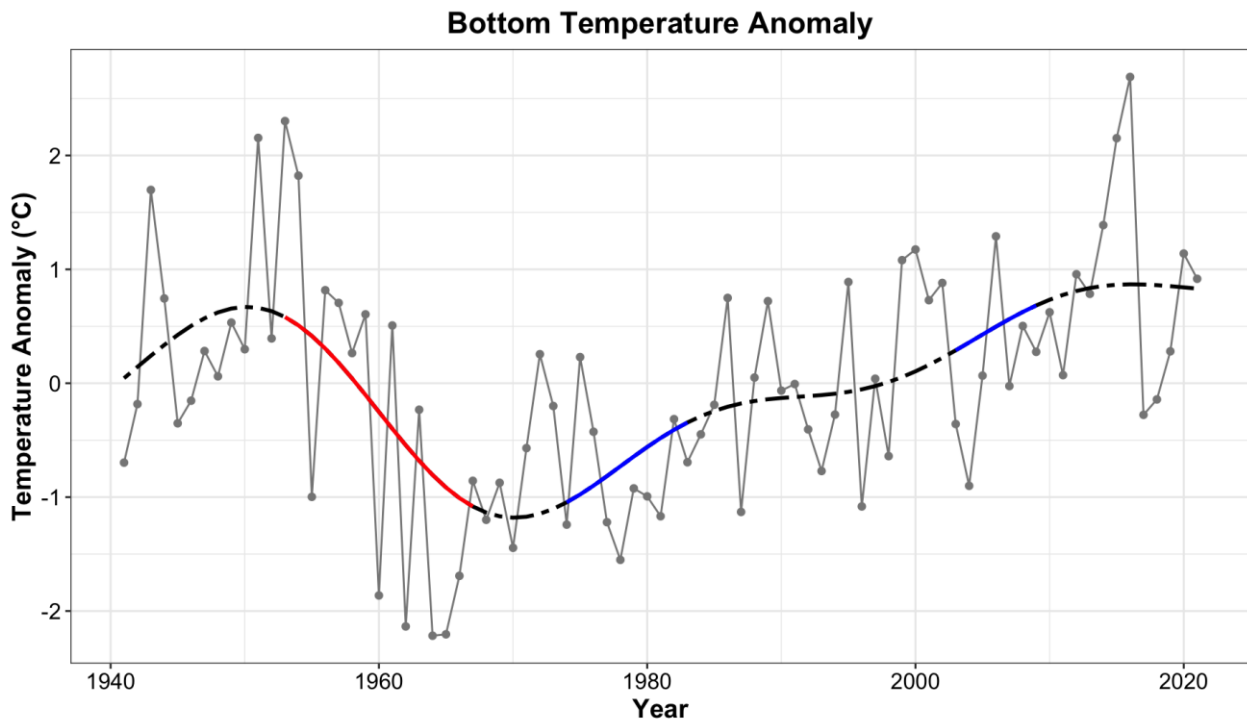


**Figure 4. Bottom temperature annual anomaly.** Grey dotted line indicates yearly values from in situ data including MBT, XBT, glider, CTD and Seawolf data. The linear trend was not significant within the 95% confidence interval and has not been included. The nonlinear GAM is shown by the dashed black line with periods of statistically significant increases in blue and decreases in red. Following a decrease during the 1950s and 1960s the bottom temperature anomaly has been steadily increasing.

### *Mid-Atlantic Cold Pool Volume and Duration*

The Cold Pool volume within the NYB region (Fig. 5) is shown during its onset (April), the middle of summer (July) and its dissolution (October). Although no statistically significant linear or nonlinear trends are present, cold pool volume in October does present interesting results. In the last decade the cold pool volume in October has been very small or zero. When compared to earlier years this could signal a shortening in duration of the cold pool with it rarely lasting into October. This is in agreement with the findings of other efforts such as the State of the Ecosystem 2022 Report for the Mid-Atlantic Region (NMFS in press), of which the New York Bight is a part. In that report the authors indicate through a persistence index that the duration of the cold pool has been shortening. We will continue to refine the indicator of Cold Pool extent, volume and duration for the New York Bight, in addition to the location of the core of the cold pool.

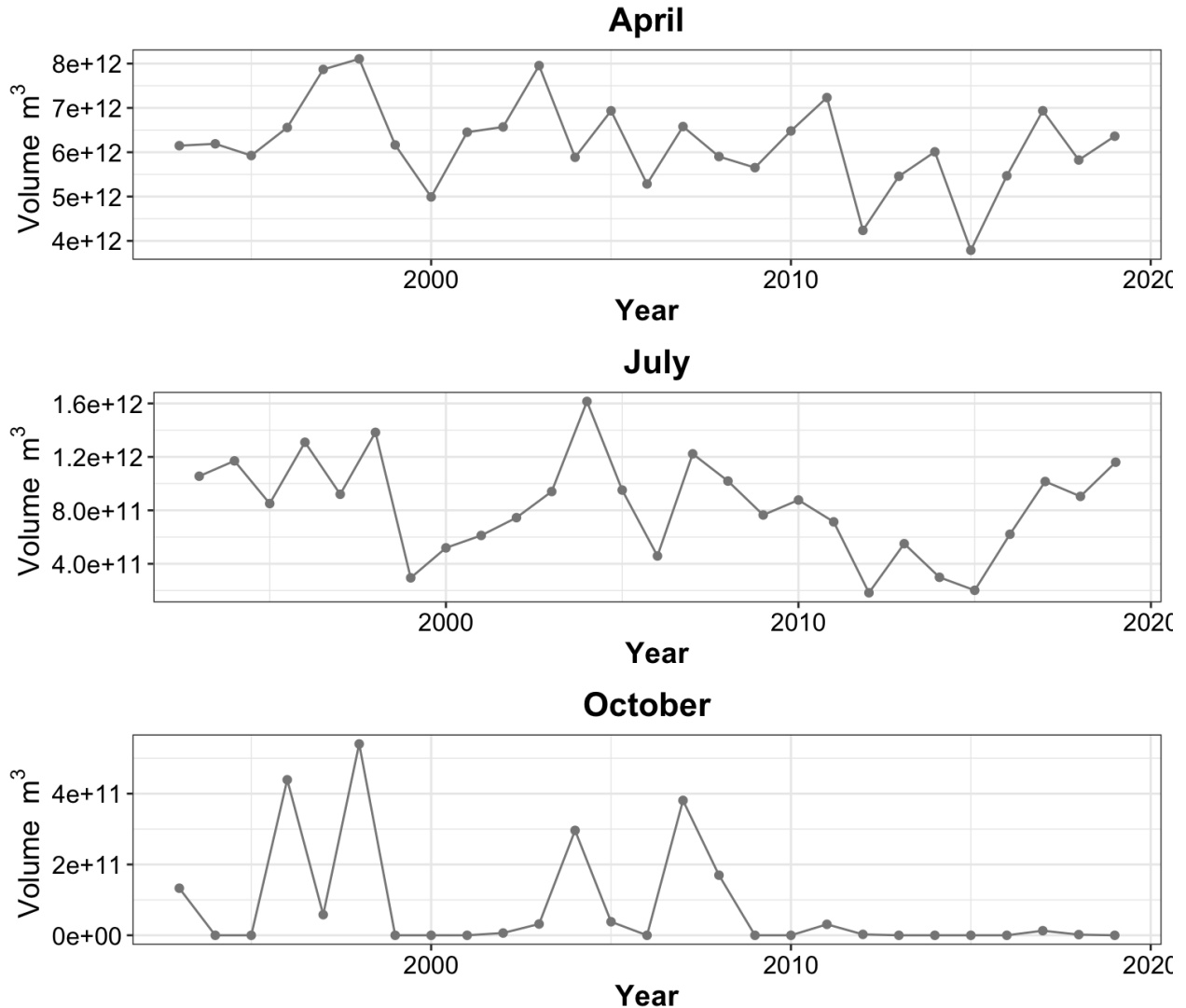


**Figure 5. Cold Pool Volume.** CP volume is shown for April (top), July (middle) and October (bottom). In all three figures the grey dotted line indicates the mean of that month during each year. Linear trends and nonlinear trends were not statistically significant and are not shown.

### **Bottom Dissolved Oxygen**

Hypoxic waters are increasing globally and have myriad of ecological effects (Diaz and Rosenberg 2008, 2009). Most consider the threshold for hypoxic waters as 2 mg O<sub>2</sub>/liter but sublethal effects of low dissolved oxygen (DO) levels occur well above this broadly accepted threshold. Ninety percent of laboratory experiments designed to assess decreases in growth and performance in marine organisms find that levels of oxygen lower than 5 mg/l cause sublethal effects such as decreases in growth, performance and/or reproductive output (Vaquer-Sunyer and Duarte 2008). Focusing our efforts on the data rich 2019 Seawolf cruise, we did not encounter any waters in the offshore area of the NYB that were below either of these biologically relevant thresholds. Thus, we use the average seasonal bottom dissolved oxygen as an indicator from our monitoring efforts (Fig. 6). The lowest dissolved oxygen values are in fall. As monitoring progresses we will report an annual index and could also develop indicators of extent and duration similar to the cold pool indicator. See Appendix for further explanation of the development of this indicator.



**Figure 6. Bottom dissolved oxygen.** The seasonal bottom dissolved oxygen from the four 2019 cruises. All DO values are greater than 5 mg/L showing that during our sampling in 2019 we did not detect hypoxic conditions in the New York Bight. Each box and whisker plots for each season shows the median (black line), 25<sup>th</sup> percentile (bottom of box) and 75<sup>th</sup> percentile (top of box) of the data. Whiskers encompass 99.3% of the data and, if present, outliers are represented by points outside the box.

### **Aragonite Saturation State and pH**

We are developing three indicators of ocean acidification in both subsurface waters and surface waters for a total of six indicators. The first is the average aragonite saturation state ( $\Omega_{\text{Ar}}$ ), and the other two are the corresponding pH and percent area of transect given some threshold of  $\Omega_{\text{Ar}}$ .

The methods are discussed in the Appendix. Although these indicators of acidification are extremely important to our interpretation of ecosystem health, lack of data prevent us from examining historical trends. This gap was identified early in the project and we prioritized collecting water samples to develop meaningful indicators. Using samples that we collected in 2019, we are able to begin to resolve seasonal variability. It is clear from the average subsurface aragonite saturation that  $\Omega_{\text{Ar}}$  and corresponding pH decreased from winter to fall, with undersaturated  $\Omega_{\text{Ar}}$  of 0.90 observed only in fall (Fig. 7, Table A1). Bottom water acidified over the course of a year, but the corresponding area of low  $\Omega_{\text{Ar}}$  shrank in fall due to the breakup of surface stratification (Table A2). At the surface we see that aragonite increased from winter to fall, likely as a function of temperature (Fig. 8). Surface pH does not have a clear trend, but is lowest in summer. With additional years of monitoring we will be able to look for annual trends and determine if the fall is indeed the season with lowest subsurface aragonite saturation states.

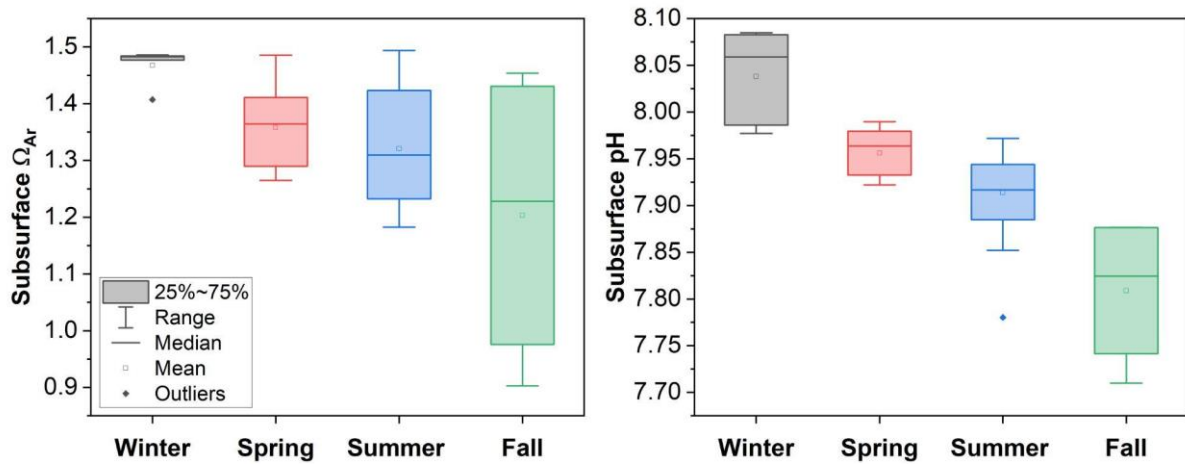


**Figure 7. Subsurface aragonite and pH.** Seasonal variation of (left) subsurface aragonite saturation state ( $\Omega_{\text{Ar}}$ ) and (right) pH in 2019. The line near the center of each box and whisker plot for each season represents the median (black line). The values at 25<sup>th</sup> and 75<sup>th</sup> percentile of the data are represented by the bottom and top of each box respectively. Whiskers encompass 99.3% of the data and, if present, outliers are represented by points outside the whiskers.

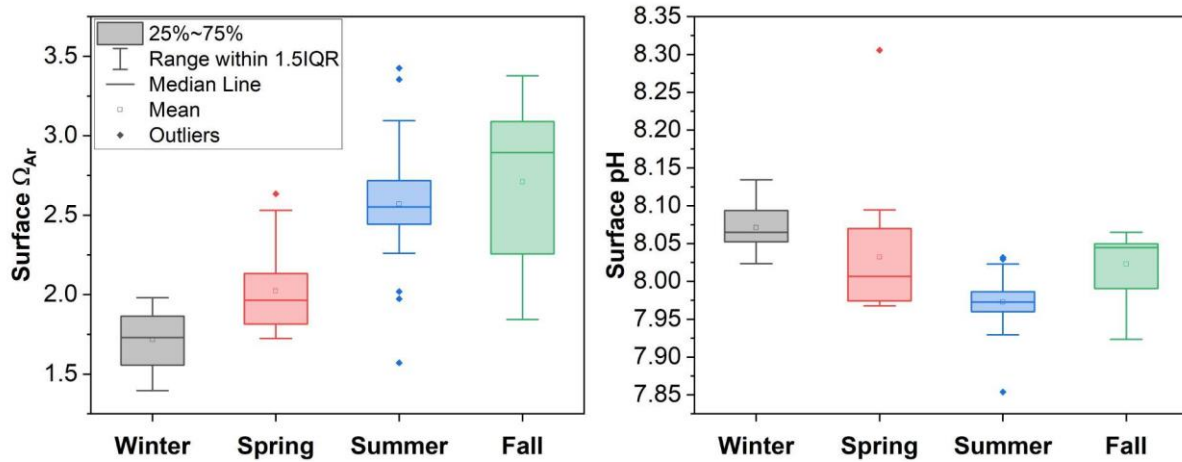


**Figure 8. Surface aragonite and pH.** Seasonal variation of (left) surface aragonite saturation state ( $\Omega_{\text{Ar}}$ ) and (right) pH in 2019. The line near the center of each box and whisker plot for each season represents the median (black line). The values at 25<sup>th</sup> and 75<sup>th</sup> percentile of the data are represented by the bottom and top of each box respectively. Whiskers encompass 99.3% of the data and, if present, outliers are represented by points outside the whiskers.

### Mean Wind Stress

Wind stress is the force exerted by the wind parallel to the surface of the water. Wind stress is important locally in determining conditions for boating and important for circulation at larger scales that can impact nutrient dynamics and other physical conditions that are important ecologically. In the NYB wind stress seems to be increasing in both spring and autumn (Fig.9).

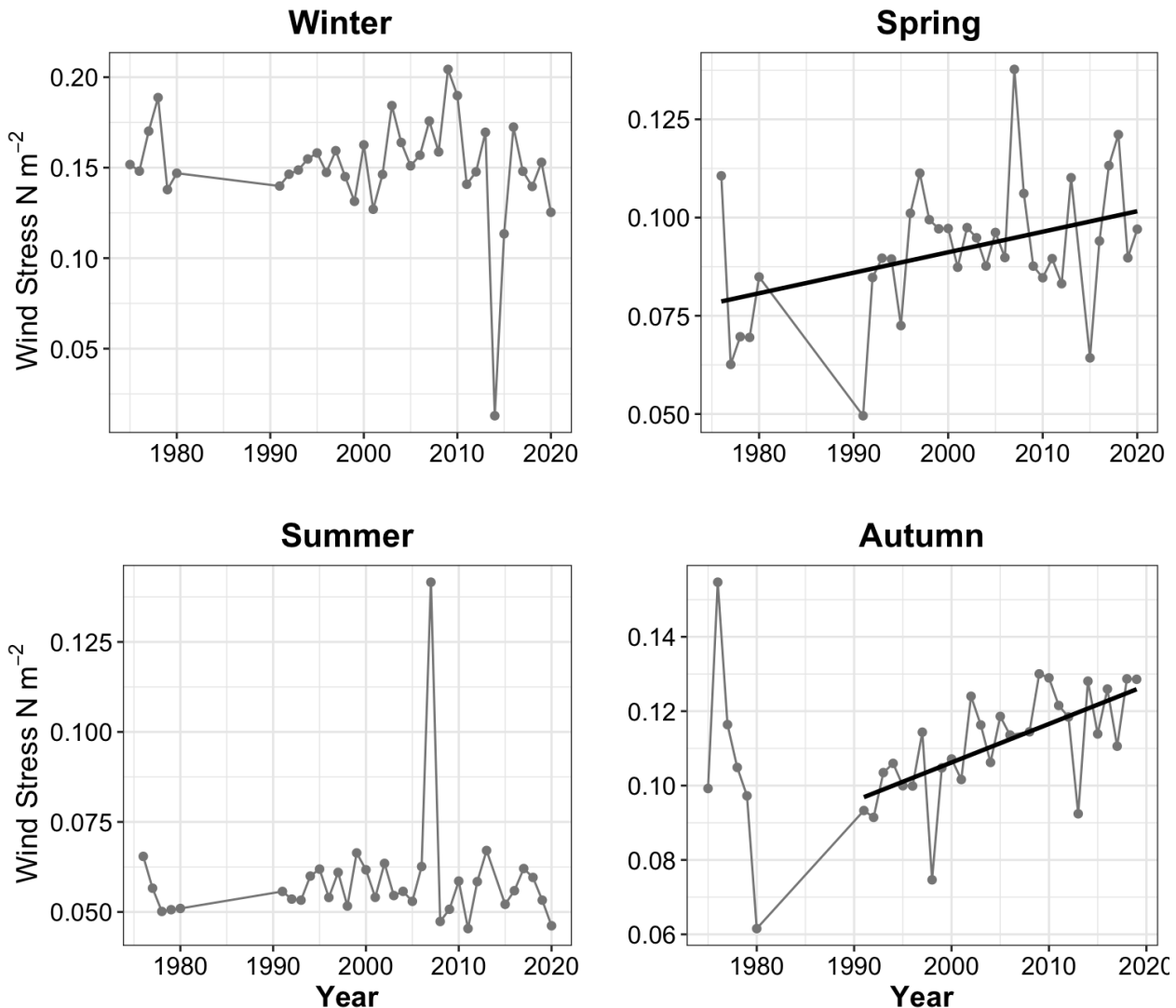


**Figure 9. Seasonal mean wind stress.** Seasonal mean wind stress as a function of wind speed, temperature, and pressure as recorded by buoy 44025 operated by the National Buoy Data Center. Winter is defined as the average of December, January, and February; Spring as March, April, and May; Summer as June, July, and August; and autumn as September, October, and November. Grey dotted lines indicate seasonal means for each year. A solid black line indicates a statistically significant linear trend, present here only in spring and autumn. Increasing wind stress is present at this buoy location during the spring and autumn months.

### *Stratification anomaly*

Differences in density caused by changes in salinity and/or temperature cause parts of the water column to be stratified or separated from each other and prevented from mixing without strong winds or other strong physical disturbance. When the water is stratified, nutrients and other small particles are generally prevented from moving vertically between layers of water. Changes in this indicator suggest changes in water mass properties. Statistically significant changes seem to have occurred around 2013, but have returned to previous levels (Fig. 10). We will investigate the causes and consequences of this change in the future.

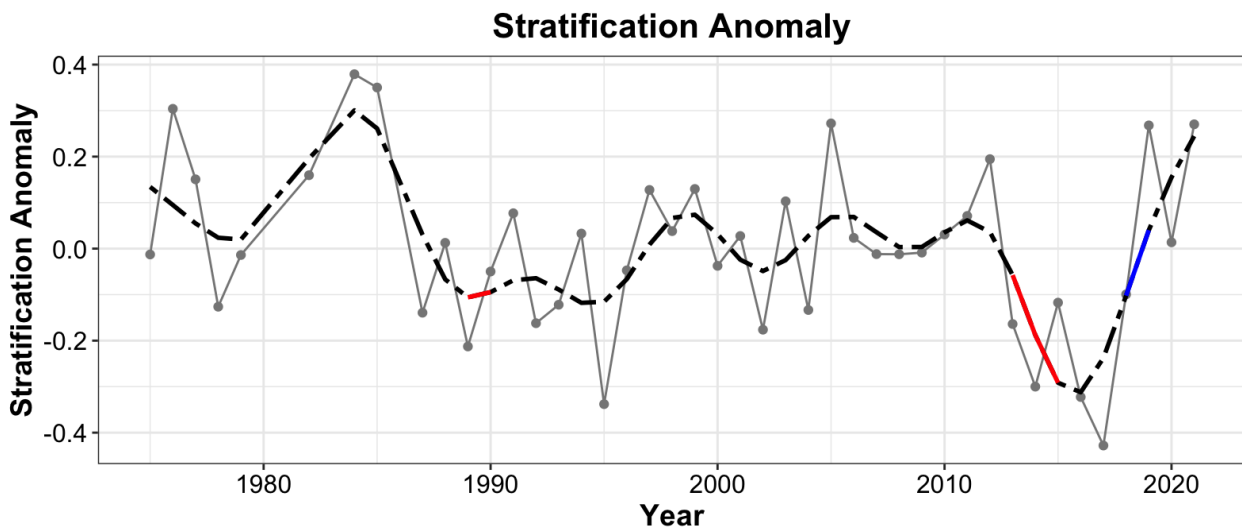


**Figure 10. Stratification anomaly.** Positive values indicating stronger stratification and negative values weaker stratification. Grey dotted line indicates the yearly values. The nonlinear GAM is shown in the dashed black line with periods of statistically significant increase shown in blue and decrease shown in red.

## Hudson River Flow

Changes in river flow may change the delivery of fresh water and nutrients to the NYB region and are usually caused by changes in precipitation. The Hudson River flow has increased over the time period that this has been recorded (Fig. 11). However, the degree to which the Hudson river outflow affects water mass properties in the NYB is unclear. The trend in Hudson river flow does not mirror the trends in stratification anomaly (Fig. 10) or salinity (Fig. 12).

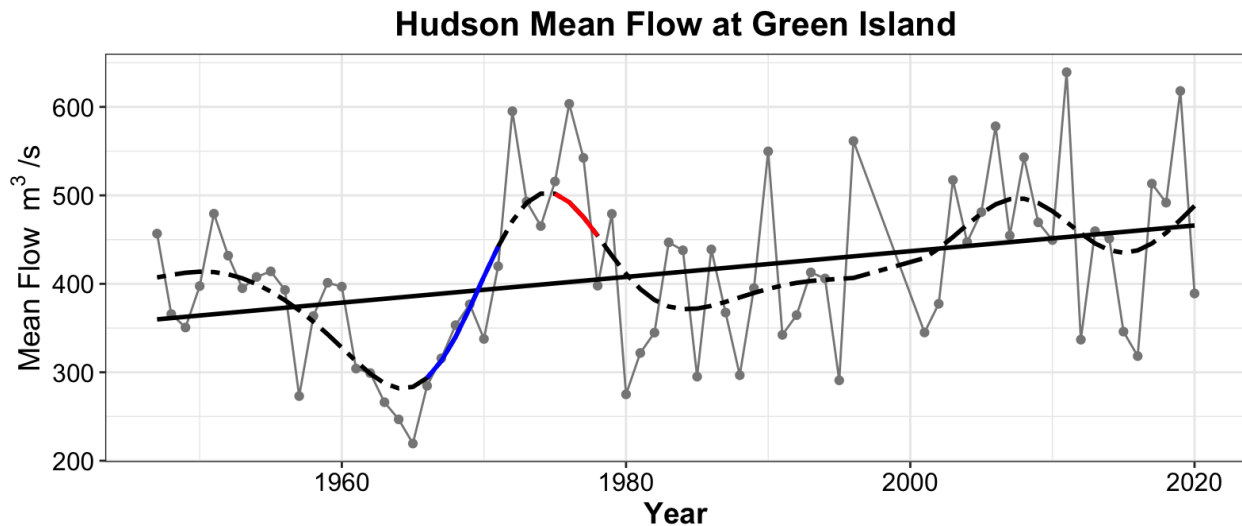


**Figure 11. Hudson River Flow.** Yearly mean Hudson River flow in  $m^3/s$  as recorded at the USGS river gauge at Green Island, NY. The grey dotted lines indicate yearly means. The solid black line shows the statistically significant linear trend. The dashed black line shows the nonlinear GAM with periods of significant increase shown in blue and significant decrease in red.

## *Salinity*

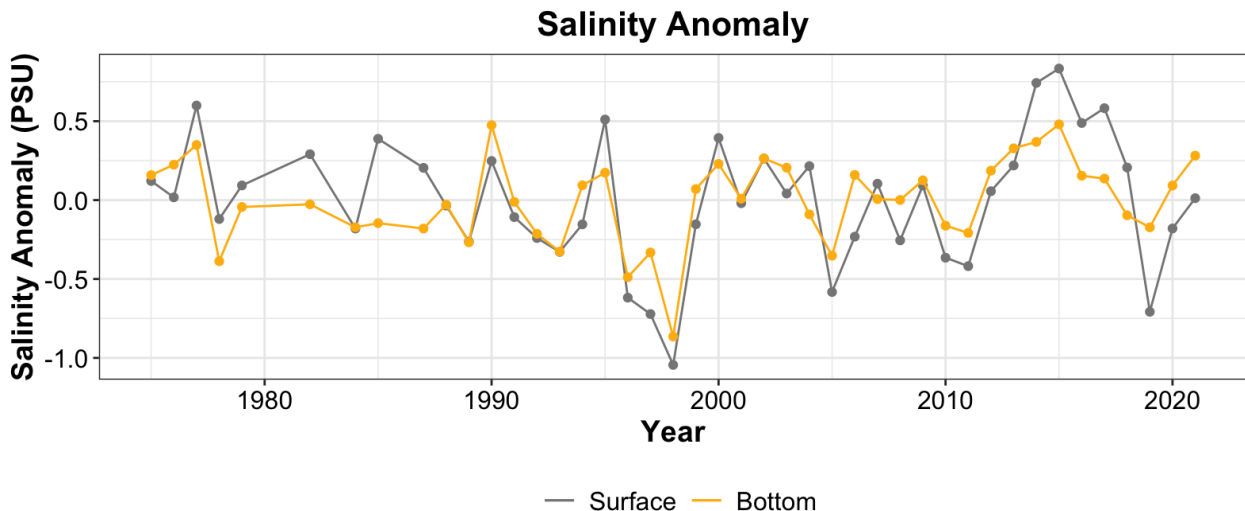


**Figure 12. Salinity anomaly.** Salinity anomalies for the surface (gray line) and the seafloor (orange line). Yearly values are shown here, no significant linear trend was present in either time series. The surface and bottom salinity anomalies are well correlated with  $r=0.77$  ( $p<0.05$ ).

## *Global Carbon Dioxide*

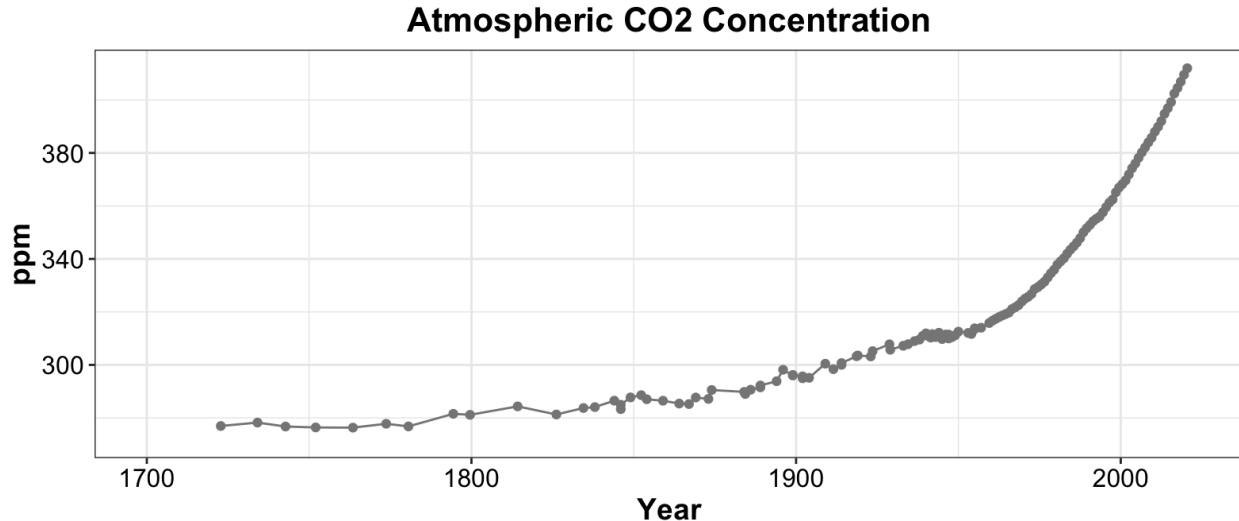


**Figure 13. Atmospheric CO<sub>2</sub> concentration.** Globally CO<sub>2</sub> concentrations have been increasing since the 1800s with an especially rapid increase since the 1950s.

### **Lobster Thermal Habitat**

American lobster supported an important fishery in New York until their collapse in the 1990s (Pearce and Balcom 2005). The movement of lobsters declines at 18.9°C and they are considered stressed above 20°C. Molting, growth, hatching success and settlement all decline at 20°C (Quinn 2017). Thus we used 20°C as the upper threshold for a productive lobster population and bottom waters greater than 20°C were considered inhospitable. We quantified the yearly mean percentage of the total NYB bottom water that is inhospitable to lobster (Fig. 14). Yearly means were calculated by averaging percent area of NYB inhospitable across all months within each year. Only a very small percentage of NYB waters fit this criteria (Fig. 15). However, water temperatures approaching this threshold may be stressful and if surface waters exceed this threshold it may impact settlement and recruitment of early life stages.

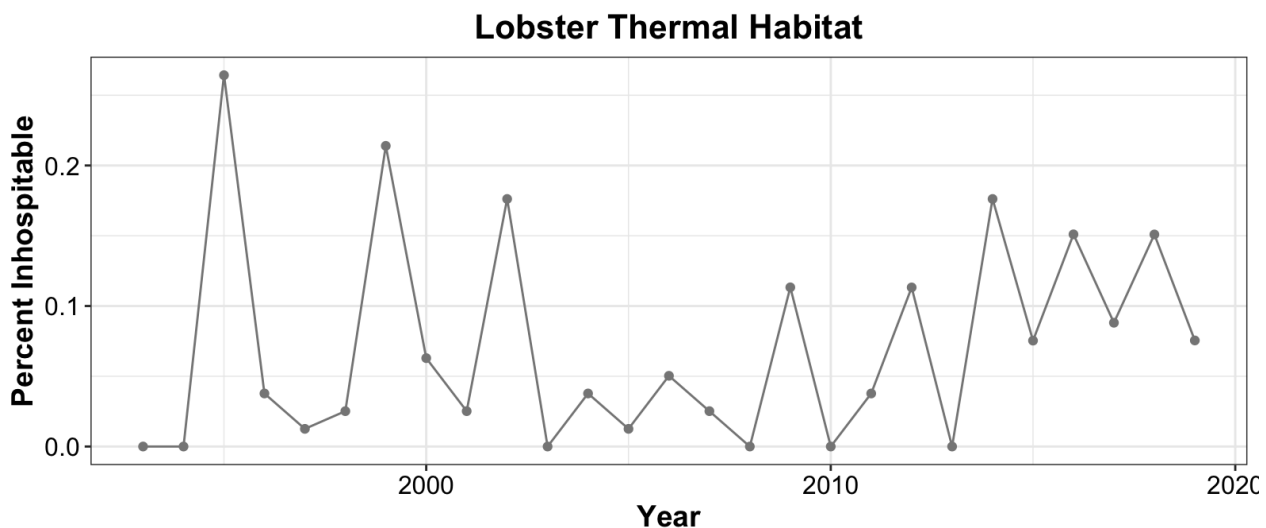


**Figure 14. Lobster thermal habitat** defined by the area of the NYB where bottom temperature is greater than 20°C.

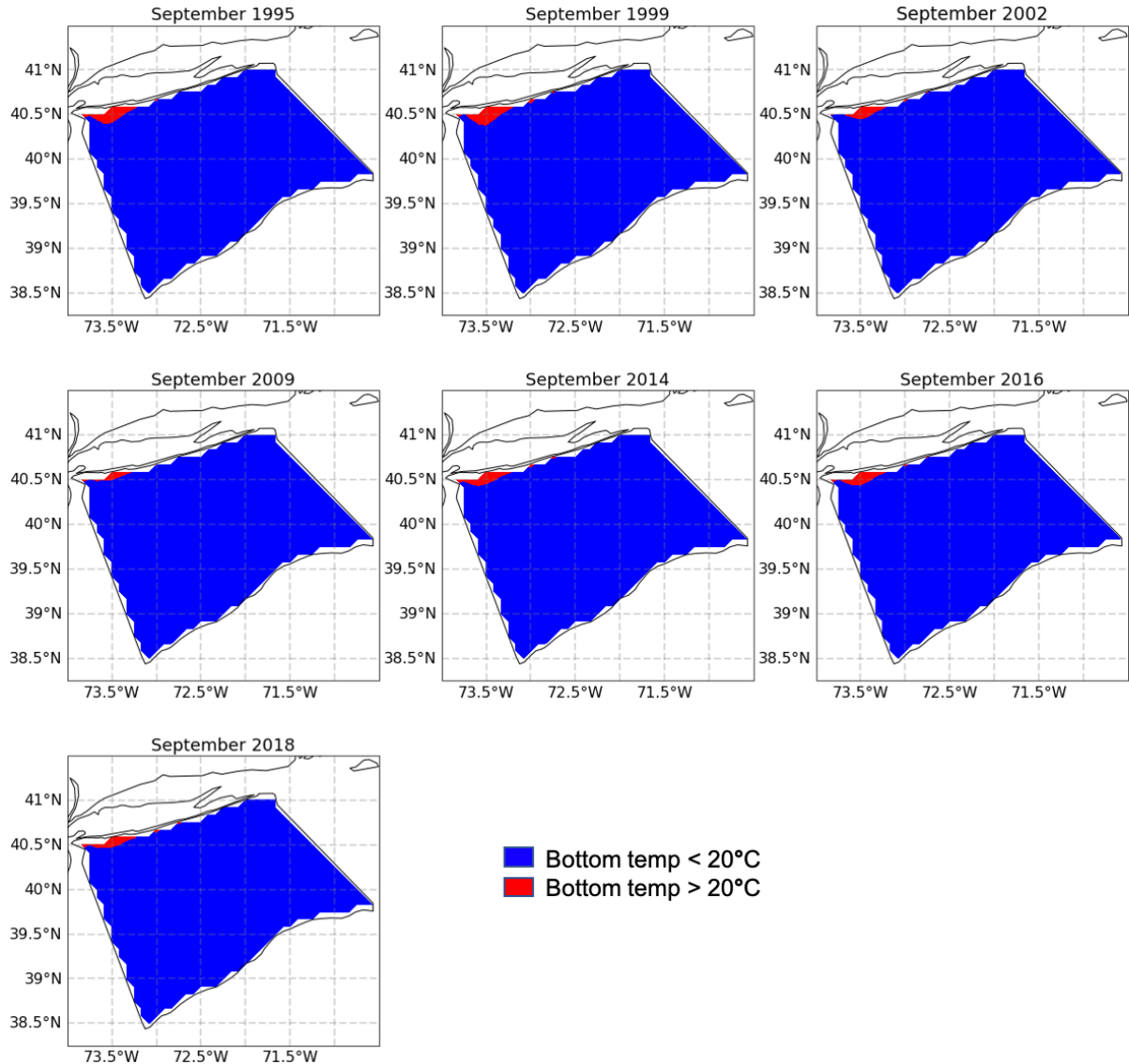


**Figure 15. Worst months for lobster.** Months when percent of area inhospitable to lobster (bottom temp  $> 20^{\circ}\text{C}$ ) was greater than 1%. Red indicates the portion of the NYB area with bottom temperature too hot for lobster, blue indicates area with acceptable temperature. All instances occurred in September indicating that lobster may be most vulnerable to rising temperatures in late summer/early fall. The largest percent area thermally inhospitable was 2.3% of total NYB area, which occurred in September of 1995 (top left).

#### Location of Surface 20°C Isotherm

As surface temperatures warm within the NYB, the location of the 20°C surface isotherm has migrated poleward. This surface isotherm is only present within the NYB during summer (JJA: June, July, August) and autumn (SON: September, October, November). During autumn (Fig. 16) this isotherm was sometimes too far south to be within the bounds of the NYB, but by the 2010s it migrated northward and was present year after year. An even more striking trend is visible in summer months (Figs. 17 and 18). The 20°C isotherm migrated northeastward from the

1980s to the 2010s and eventually out of the NYB region all together, leaving surface warmers warmer than 20°C within the NYB during summer of the most recent years.

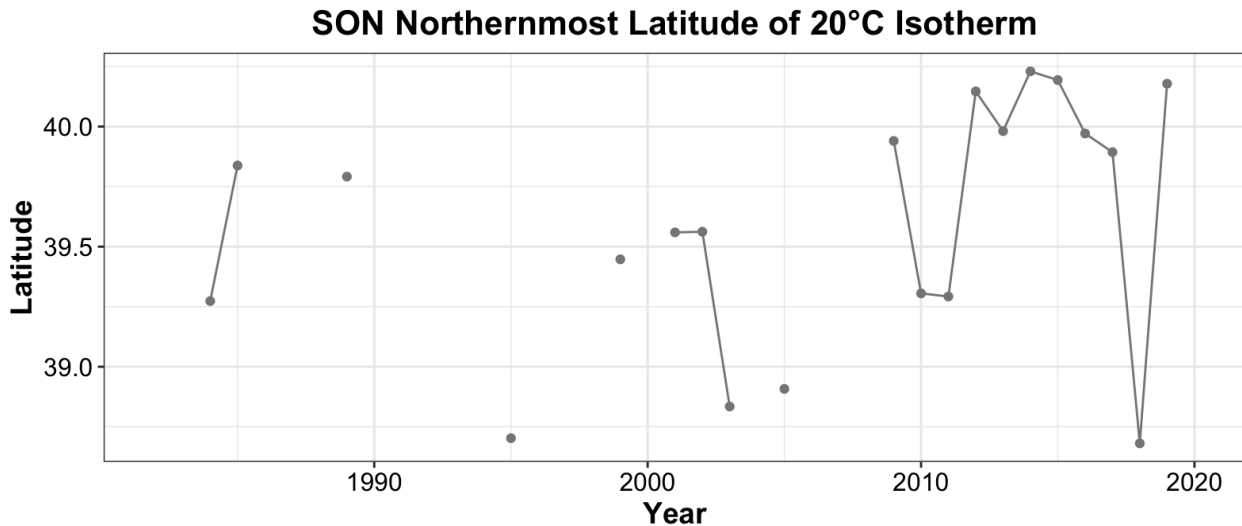


**Figure 16. Autumn 20°C surface isotherm.** Northernmost latitude of the 20°C surface isotherm within the NYB area during autumn (SON: September, October, November). Dark grey dotted line indicates yearly means of autumn months. Years without any data indicate that the 20°C isotherm was still south of the NYB area.

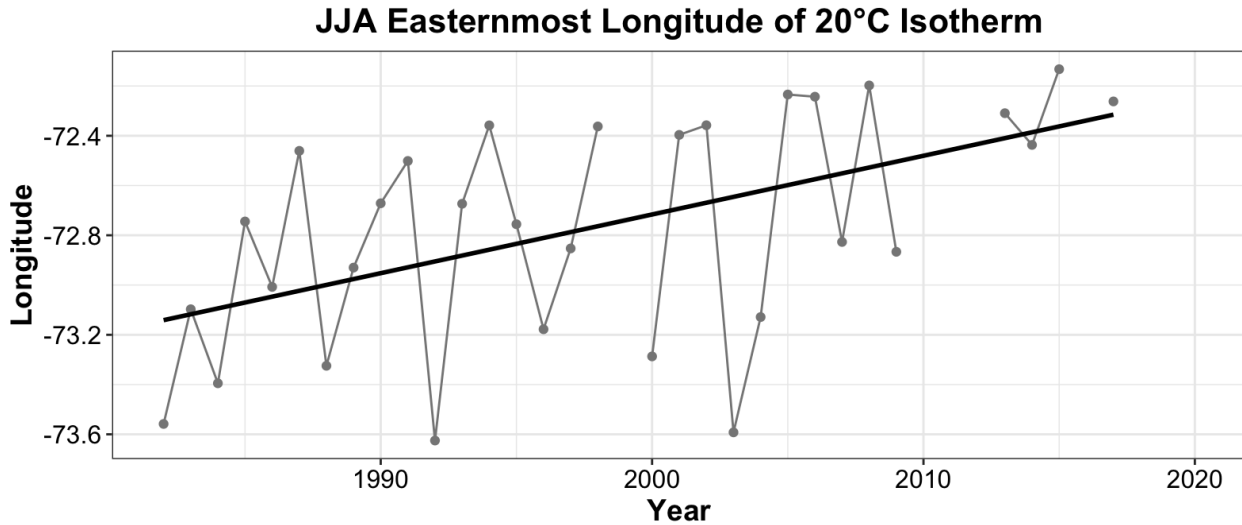


**Figure 17. Summer 20°C surface isotherm.** Easternmost longitude of the 20°C surface isotherm within the NYB area during summer (JJA: June, July, August). Dark grey dotted line indicates yearly means of summer months. The solid black line shows the statistically significant linear trend. Years without data indicate that this isotherm was so far to the northeast that it was no longer within the NYB area.

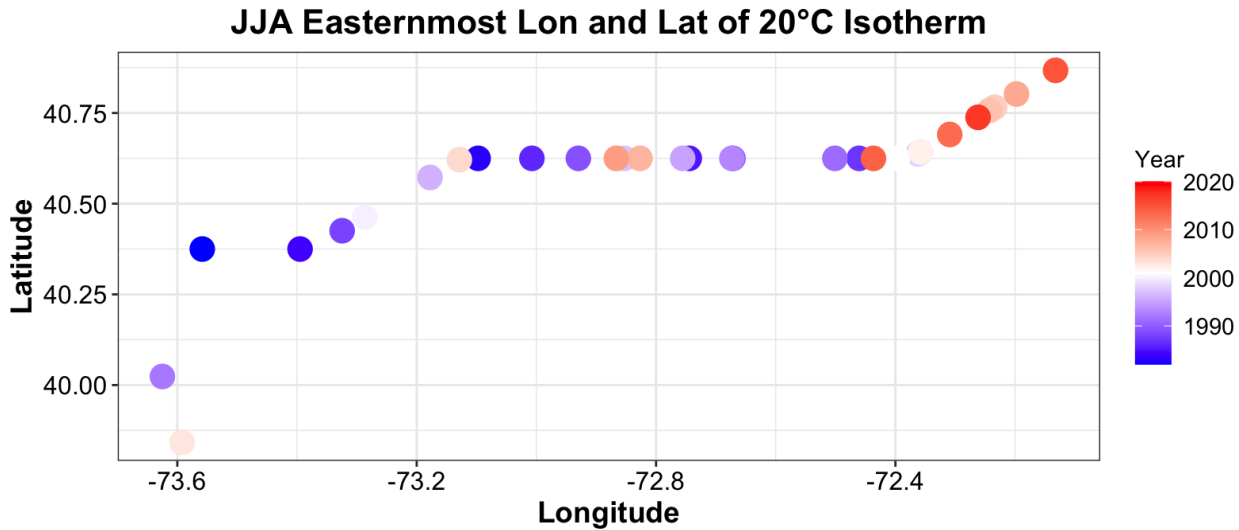


**Figure 18. Summer 20°C isotherm location.** The longitude and latitude of the easternmost point of the 20°C surface isotherm during summer months. The color of the point indicates its year. Since the 1980s this isotherm has been moving northeastward, and eventually out of the NYB leaving summer surface waters warmer than 20°C.

### Summary for Physical and Chemical Indicators

When all the physical indicators are tested for correlations with one another some patterns emerge (Fig. 19). Many of the SST based indicators such as seasonal mean sea surface temperature, marine heatwave days, and location of the surface 20°C isotherm are positively correlated with each other. This is unsurprising, as we are seeing a warming trend across all seasons that can also be seen in the poleward (northward during SON, northeastward during JJA) shift in surface isotherms, as well as a simultaneous increase in marine heatwave days during the last decade. We found that the transition to summer sea surface temperatures occurs earlier and the transition to autumn sea surface temperatures also occurs later, making the length of summer, the warmest time of the year on the shelf, much longer. A similar trend has been observed across the Northeast shelf where spring occurs slightly earlier and the fall transition occurs much later effectively making summer longer (Henderson et al. 2017, Thomas et al. 2018). This trend was strongest at northern latitudes (Gulf of Maine) and weakest at the southern edge of this ecosystem (Thomas et al. 2018) and affected the distribution of pelagic fishes and the biomass of benthic fishes with a lag of a few years (Henderson et al. 2017) so we investigated this trend for the NYB specifically. We found that the trend in transition from summer to fall was much more pronounced than the slight trend in the spring.

Cold pool volume shows statistically significant correlation with many of the temperature and salinity indicators. The largest correlations occur between the CP volumes and SST in the spring, bottom salinity, and bottom temperature. That these correlations are negative relates to the definition of the cold pool as the region bounded by waters at or below 10°C and 34 PSU. Therefore, lower salinity and temperature trends would likely be associated with increasing trends

in cold pool volume. The cold pool volume in the fall is also negatively correlated with the fall wind stress indicator. We noted earlier in the report that in recent years the cold pool appears to be shortening in duration, often completely dissolving by October. This correlation with fall wind stress could indicate that increasing autumnal winds may play a role in increasing mixing and breaking down the stratification that forms the cold pool.

Further analysis of anomalous years in seasonal wind stress time series, as well as potential implications of increasing Hudson River flow on NYB ecosystems will be presented in subsequent reports. Although 2019 data indicates that hypoxia conditions were not present in the NYB, we look forward to increased data availability from upcoming field work so we may assess year to year trends in DO as well as acidification indicators. In particular, we will examine if the combined stressors of low DO, low aragonite saturation state and high temperatures in bottom water are stressful to marine organisms, especially shellfish.

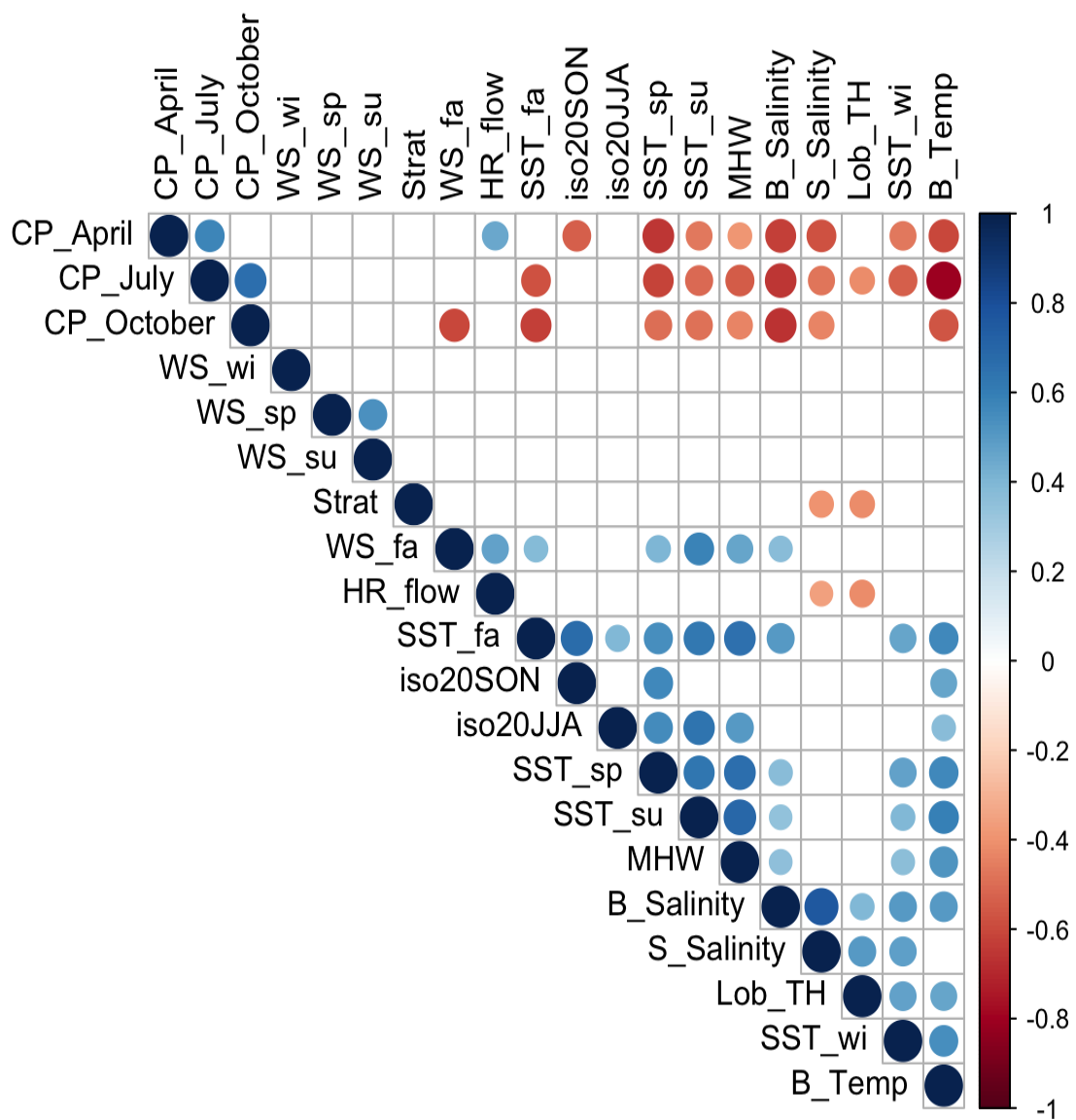


**Figure 19. Pairwise correlations of physical indicators.** Correlations between physical indicators with blank squares indicating non-significant ( $p>0.05$ ) correlations. Blue indicates a positive correlation while red indicates a negative correlation. The size of the circle as well as the color shading indicate the magnitude of the  $r$  value, with large values shown in deeper reds and blues and bigger circles.

## 4. Marine Community

### *Monthly mean surface chlorophyll*

Surface chlorophyll concentrations tend to be highest in the late autumn, specifically November. Surface chlorophyll is not necessarily directly correlated with primary productivity. Although summer months such as June and July appear to show low chlorophyll concentrations, primary productivity may in fact be quite high but associated with a subsurface chlorophyll maximum which may not be identified by satellite data.

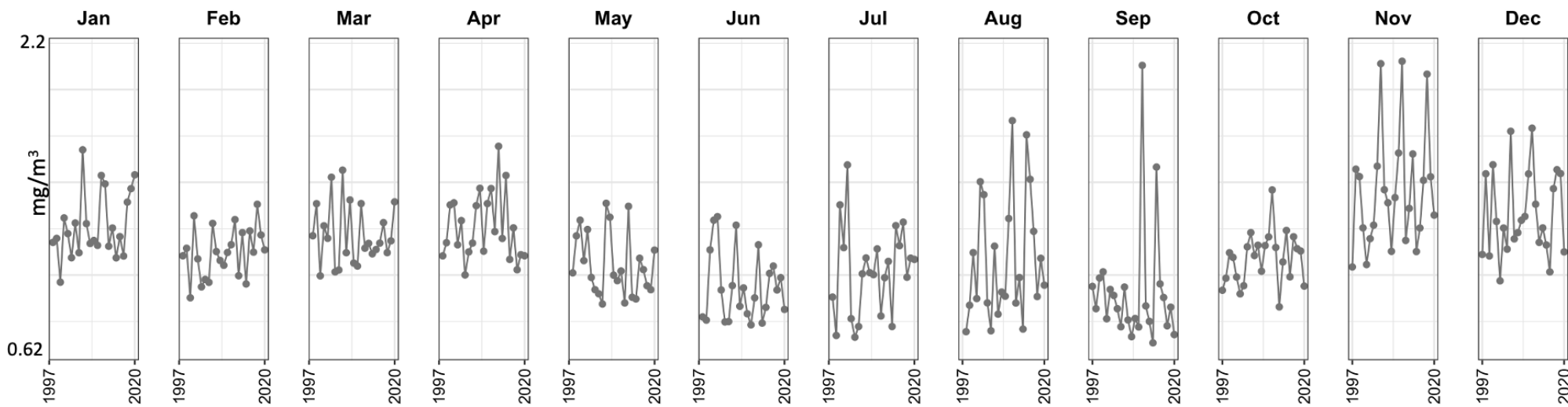


**Figure 20. Monthly mean surface chlorophyll.** Monthly mean surface chlorophyll-a concentration in  $\text{mg}/\text{m}^3$  from satellite data. Dark grey dotted lines show monthly means across the NYB area for each year from 1997 through 2020.

### *Calanus finmarchicus* abundance

*Calanus finmarchicus* is one of the largest and most abundant copepods in the Northwest Atlantic. It is an extremely important prey item for many marine organisms including the endangered North Atlantic right whale because of its rich lipid stores. It is considered a cold water zooplankton species so declines in abundance are an indicator of warming temperatures. It has been steadily declining since 2005 when it reached its highest abundance in the NYB, but its lowest abundance was in 1991 (Fig. 21).

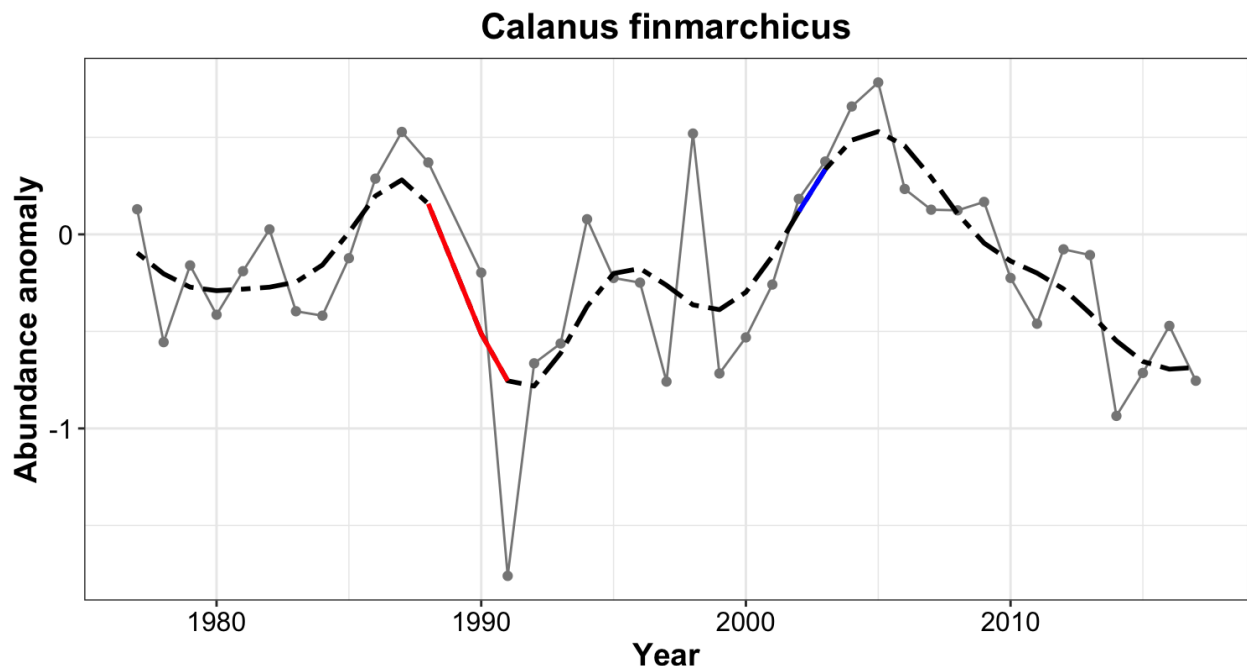


**Figure 21. *Calanus finmarchicus*.** Abundance anomalies of *Calanus finmarchicus*. The dark grey dotted line indicates yearly means. The dashed black line shows the nonlinear GAM with periods of statistically significant increase in blue and decrease in red. No significant linear trend was found.

### Copepod size index

The ratio of small to large copepods is largely driven by changes in the large *Calanus finmarchicus*, but also considers all of the most common species of copepods in the NYB. A change from large to small zooplankton can signal a decline in fisheries production and the efficiency with which energy flows from primary production to benthic and pelagic fishes (Stock et al. 2017). This ratio was lowest in 2005 and has been increasing since then.

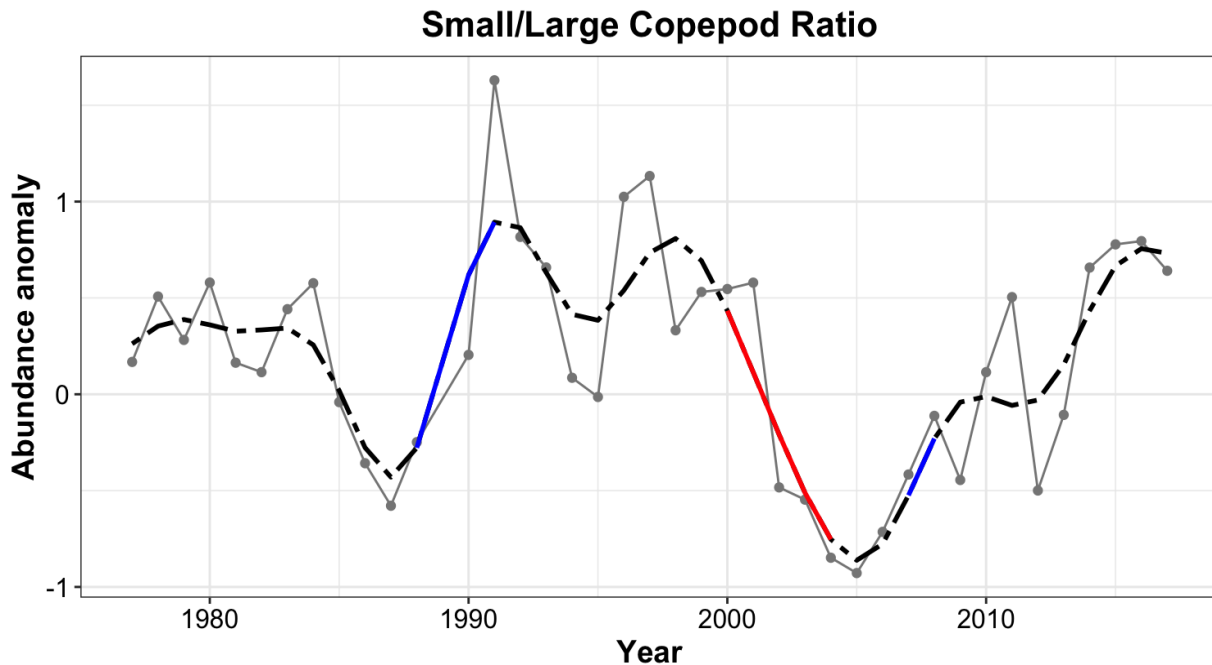


**Figure 22. Small/large copepods.** The ratio of small to large copepods is shown with dark grey points indicating yearly means. The dashed black line is the nonlinear GAM with periods of significant increasing trend in blue and decreasing trend in red. No significant linear trend was found. The abundance of *Calanus finmarchicus* in the NYB is a likely driver of the small/large copepod ratio anomaly.

### Commercially important invertebrate biomass

American lobster was an important fishery in New York that collapsed in the 1990s. Its abundance has been generally declined as indicated by the NEFSC bottom trawl survey in the fall and has been sporadic in the spring (Fig. 23). Coastwide landings of Jonah crab fishery have increased dramatically in recent years, but have decreased in NY recently. This species has only been regulated in Federal waters since 2019. Jonah crabs appear to have declined in spring trawl surveys, but increased in fall surveys (Fig. 23). Longfin squid are one of the most important commercial fisheries in NY. The NOAA NEFSC bottom trawl survey indicates a strong declining trend in spring, but steady abundance in the fall survey (Fig. 24), but no trend emerges with shortfin squid (Fig. 24). The divergent trends in spring and fall for each of these species are likely a result of temperature-dependent availability to the survey.

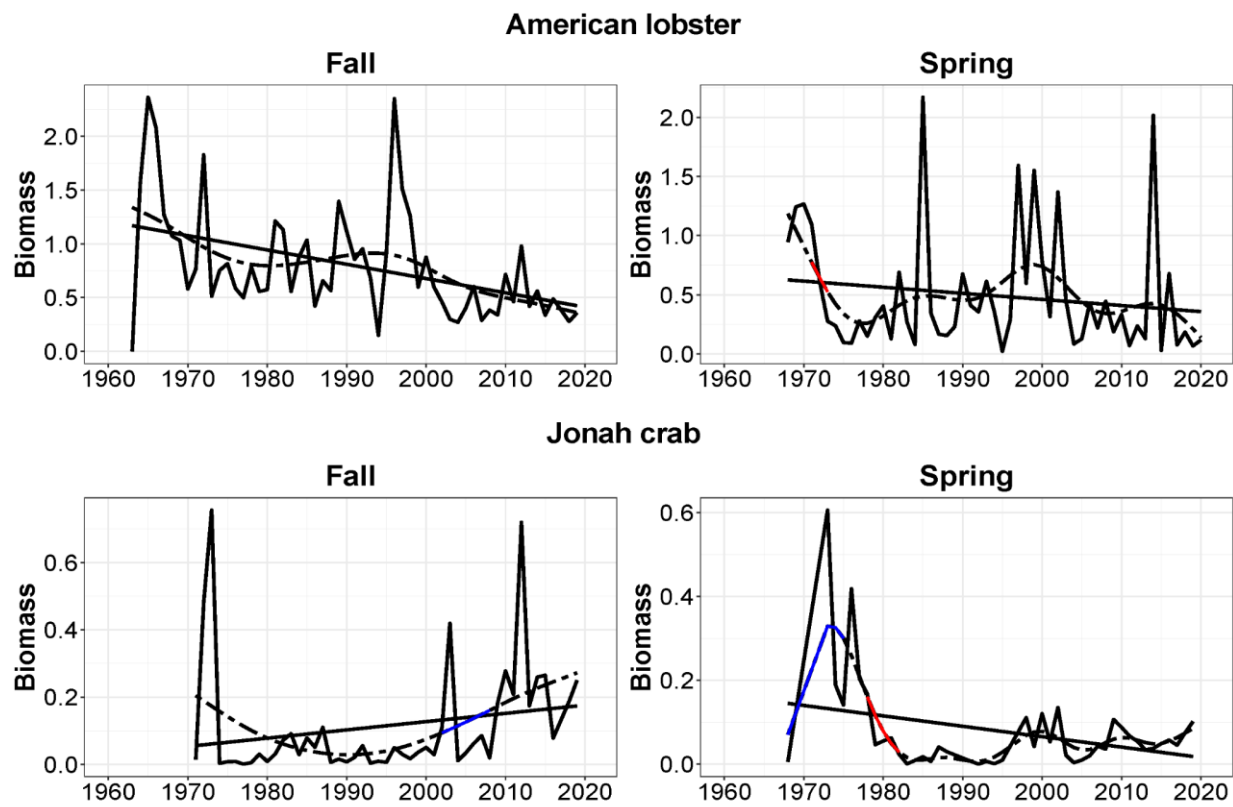


**Figure 23. American lobster and Jonah crab.** Mean stratified biomass of American lobster and Jonah crab in the fall (left) and spring (right) NOAA NEFSC trawl survey. These species are commercially important to NY communities. The dashed black line is the nonlinear GAM with periods of significant increasing trend in blue and decreasing trend in red. The linear trend is shown, but is only statistically significant if shown in red (decreasing linear trend) and blue (increasing linear trend) colors.

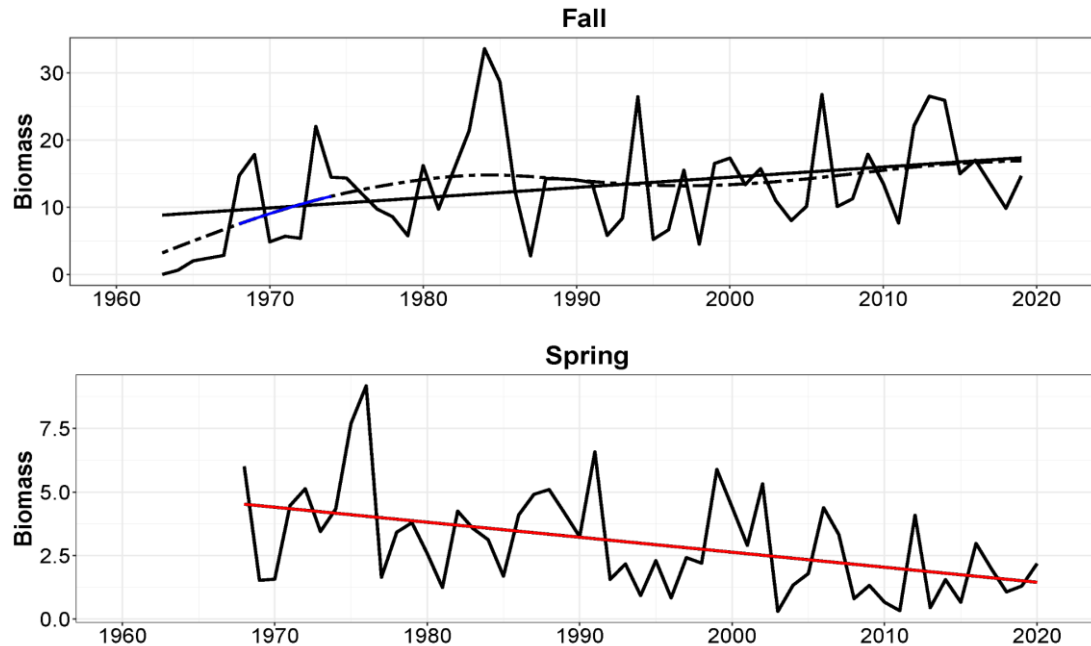


**Figure 24. Longfin squid biomass.** Longfin squid biomass in the fall (top) and spring (bottom) in the NOAA NEFSC bottom trawl survey. The dashed black line is the nonlinear GAM with periods of significant increasing trend in blue and decreasing trend in red. The linear trend is shown, but is only statistically significant if shown in red (decreasing linear trend) and blue (increasing linear trend) colors.

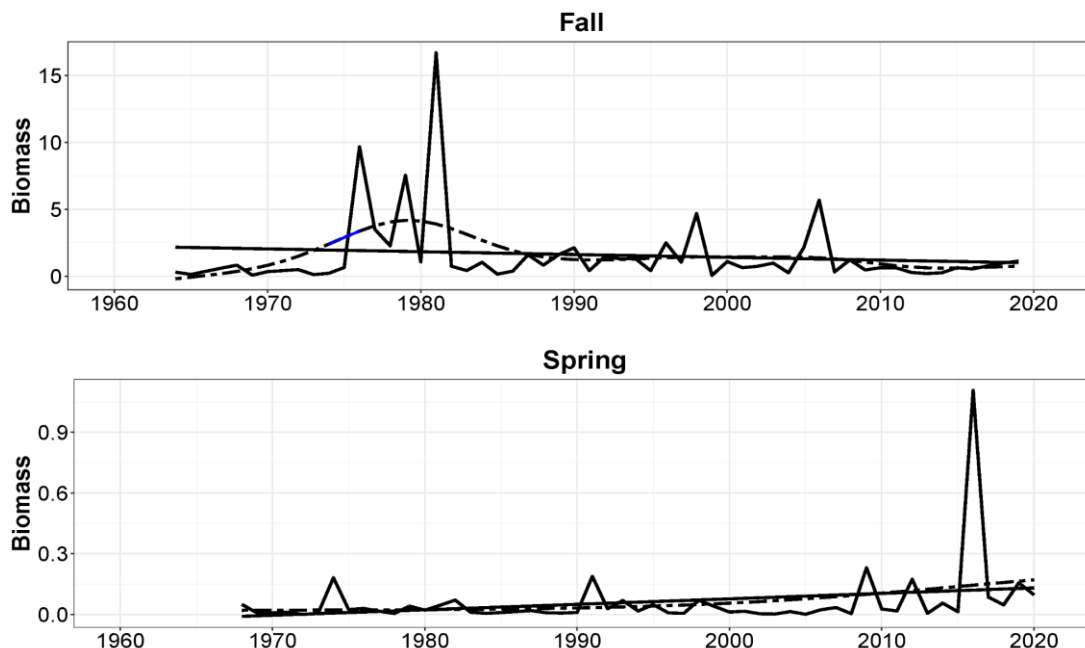


**Figure 25. Northern shortfin squid biomass.** Northern shortfin squid biomass in the fall (top) and spring (bottom). The dashed black line is the nonlinear GAM with periods of significant increasing trend in blue and decreasing trend in red. The linear trend is shown, but is only statistically significant if shown in red (decreasing linear trend) and blue (increasing linear trend) colors.

### *Forage species biomass*

Forage species are important prey for economically important fish species as well as protected species like marine mammals. Although there may have been changes in biomass of individual species, there has been no significant change in their biomass as a whole in the NYB in recent years (Fig. 26). This indicator currently only includes forage fishes, but in the future will include squid and potentially other pelagic invertebrates as forage species.

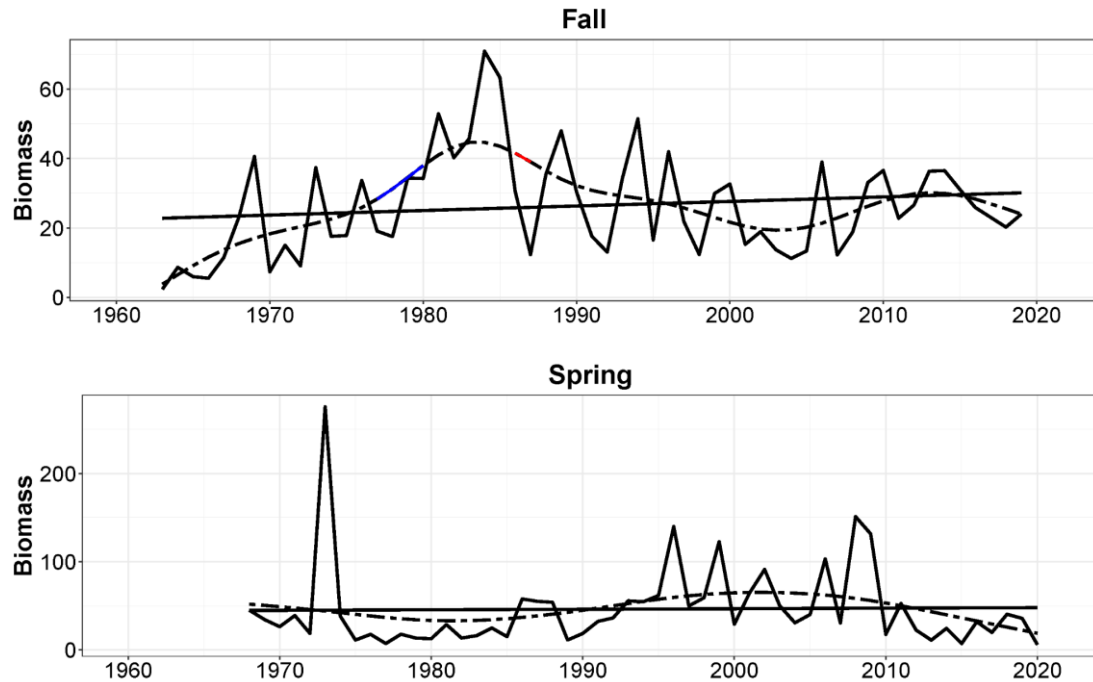


**Figure 26. Forage species biomass.** Forage species biomass is estimated from the fall (top) and spring (bottom) NOAA NEFSC bottom trawl survey. The dashed black line is the nonlinear GAM with periods of significant increasing trend in blue and decreasing trend in red. The linear trend is also indicated by the solid black line, but similar to the nonlinear GAM trends statistical significance is indicated only by red (decreasing) and blue (increasing) colors.

### *Aggregate Feeding groups*

In addition to looking at each individual species, we developed indicators of broad trophic groups to assess ecosystem health with respect to middle trophic level species. While individual species may decline, in a resilient ecosystem a complimentary species within the same trophic group could increase to fill its niche. Changes in biomass within a trophic group may indicate changes in the energy flow and food web structure that may impact total system production and ecosystem resilience. To examine this concept, we used the same trophic groups as defined by NOAA in their Ecosystem Status Report (NMFS 2021). Benthic organisms have increased while piscivores have decreased (Fig. 27), suggesting major changes in the food web over the last 60 years. We also looked at total trawl biomass (Fig. 28). Biomass declined early in the time series in the fall

likely as a result of fishing large piscivores, but spring biomass has fluctuated quite a bit on a roughly decadal time scale.

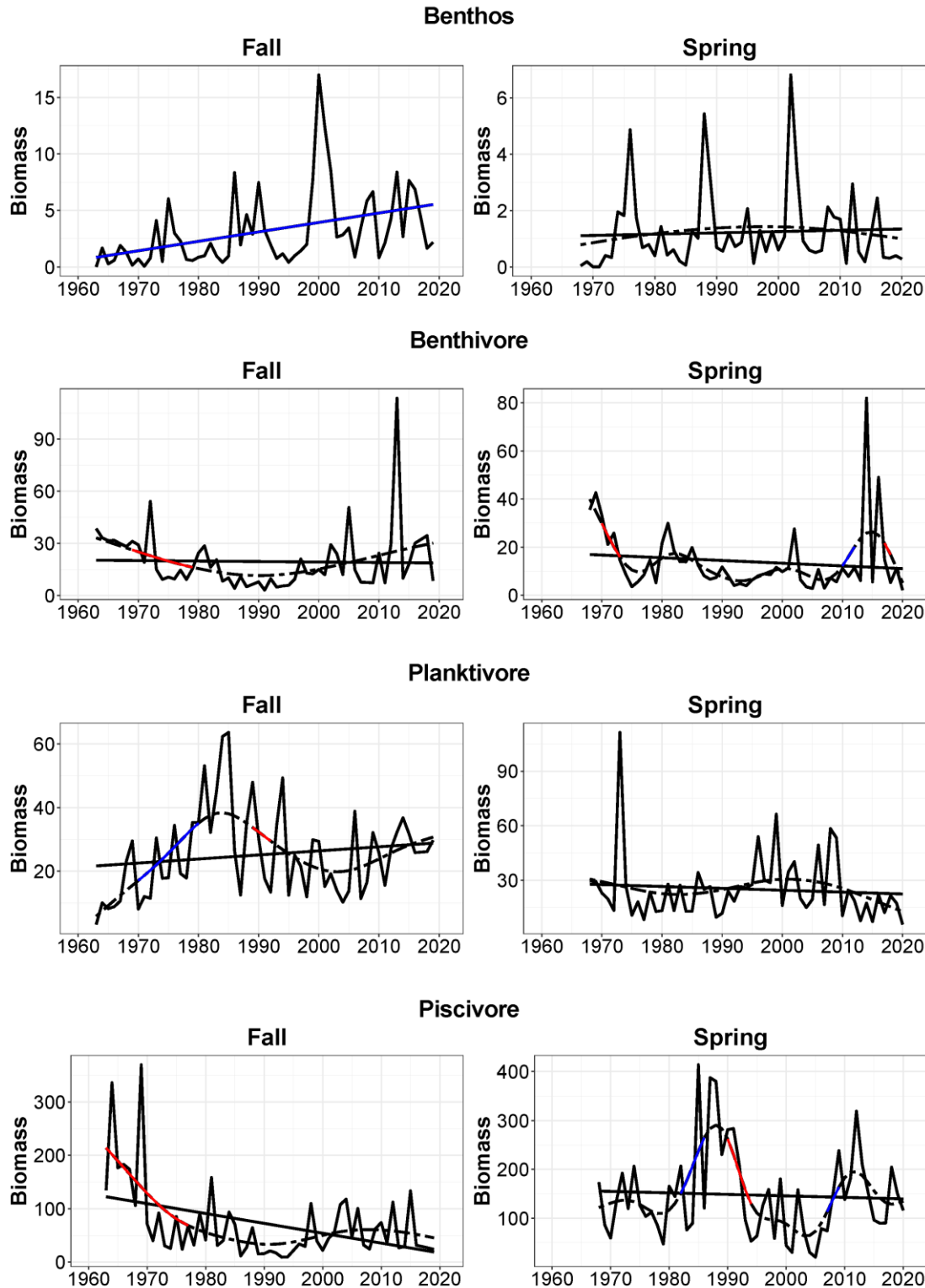


**Figure 27. Biomass of fish trophic groups.** Biomass (kg/tow) from fish trophic groups during fall (left) and spring (right) from NOAA NEFSC bottom trawl surveys. The dashed black line is the nonlinear GAM with periods of significant increasing trend in blue and

decreasing trend in red. No significant linear trend was found. The blue line in fall benthos graph appears linear, but is a significant trend fitted with a GAM.

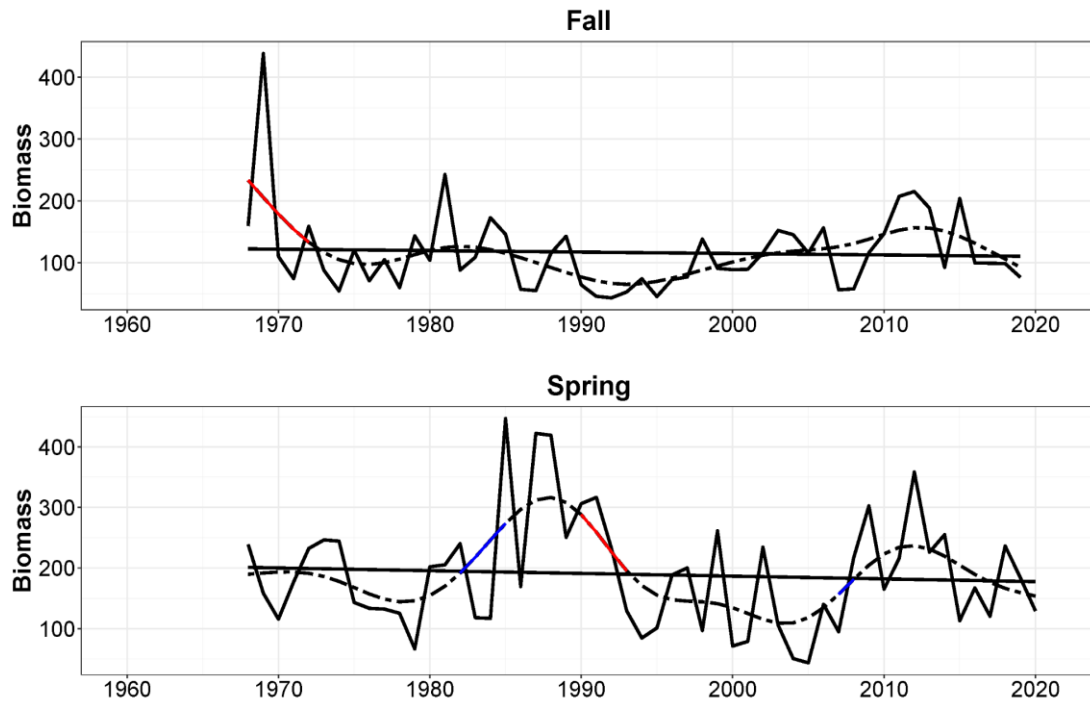


**Figure 28. Total trawl biomass.** The y axis shows total metric tons of fish and macroinvertebrates captured in the fall (top) and spring (bottom) NOAA NEFSC bottom trawl surveys. The dashed black line is the nonlinear GAM with periods of significant increasing trend in blue and decreasing trend in red. No significant linear trend was found.

#### *Northern vs. Southern finfish and macroinvertebrates*

Black sea bass and summer flounder are two piscivorous fishes that are important commercially and recreationally. Black sea bass is a temperate grouper species with a wide distribution along the east coast of the US. It is an important commercial fishery and one of the top five most important recreational fisheries in New York. Summer flounder is an important commercial fishery and consistently one of the top five most important recreational fisheries in New York. The abundance and biomass of both species has increased in the last decade and this is thought to be related to warming coastwide temperatures (Fig. 30, 31). In particular, black sea bass biomass is an order of magnitude higher than it was in the early part of the time series. After being overfished, it recovered due to good management and environmental conditions conducive to growth and recruitment for this species. The ratio of northern to southern species is based on the historical occurrence of each species in the NOAA NEFSC trawl survey from 1963-2000. If the biomass-weighted mean latitude was greater than  $39.6^{\circ}$  latitude it was labeled a “northern” species and all others were considered “southern” species. This threshold latitude lies roughly at New Egg Harbor, NJ and in the future different thresholds could be evaluated. Despite the increase in two southern species (black sea bass and summer flounder), there does not seem to be

a recent decline in the ratio of northern to southern species (Fig. 31). The largest change in this indicator actually occurred with the overfishing that occurred in the 1960s and 70s.

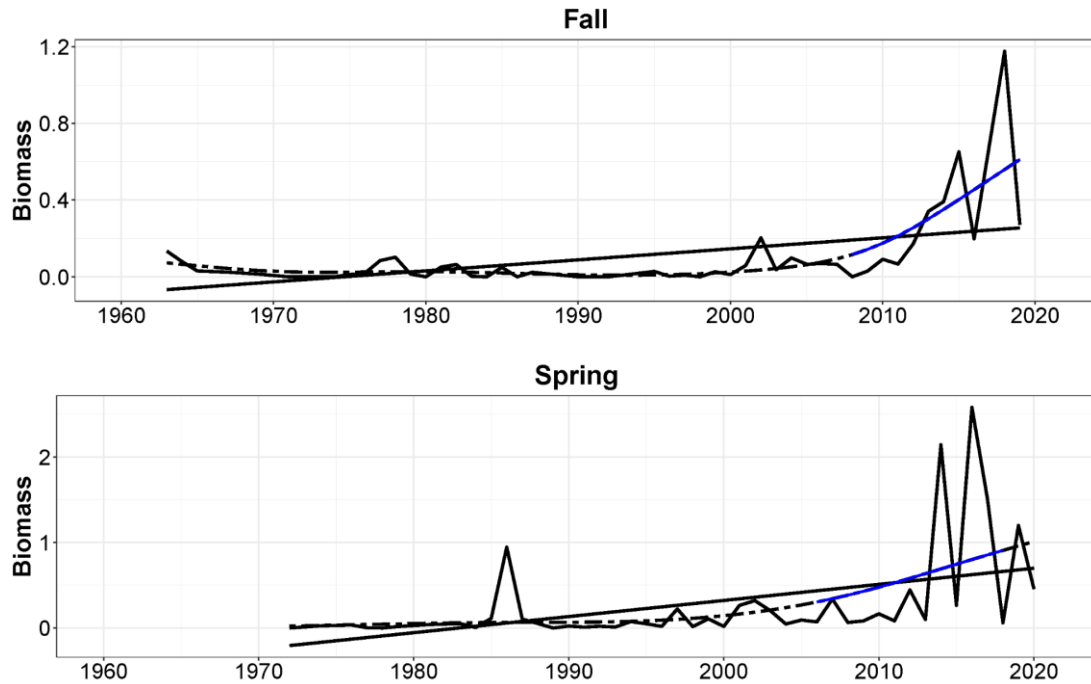


**Figure 29. Black sea bass biomass.** The values shown are mean stratified biomass (kg/tow). The dashed black line is the nonlinear GAM with periods of significant increasing trend in blue. No significant linear trend was found.

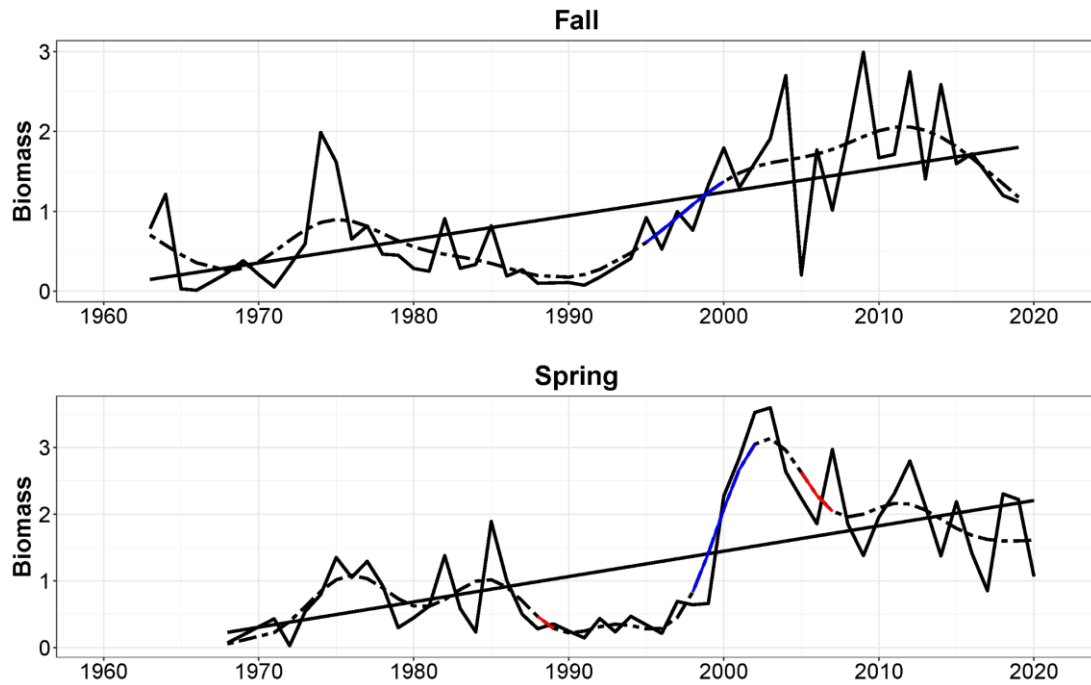
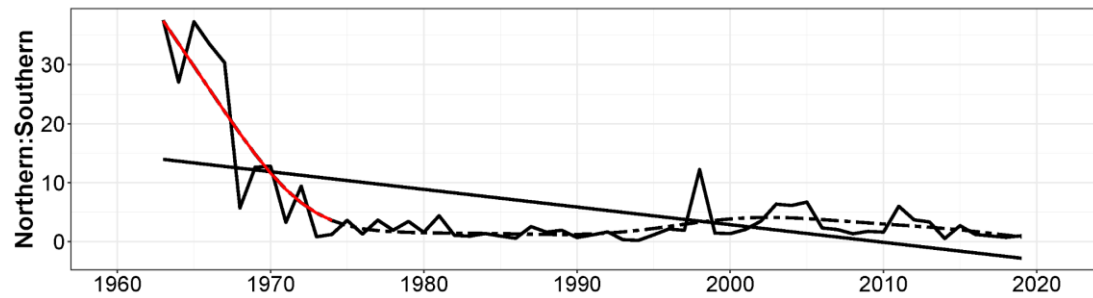


**Figure 30. Summer flounder biomass.** The values are mean stratified biomass (kg/tow). The dashed black line is the nonlinear GAM with periods of significant increasing trend in blue and decreasing trend in red. No significant linear trend was found.

*Ratio of Northern to Southern species biomass*

Fall



Spring

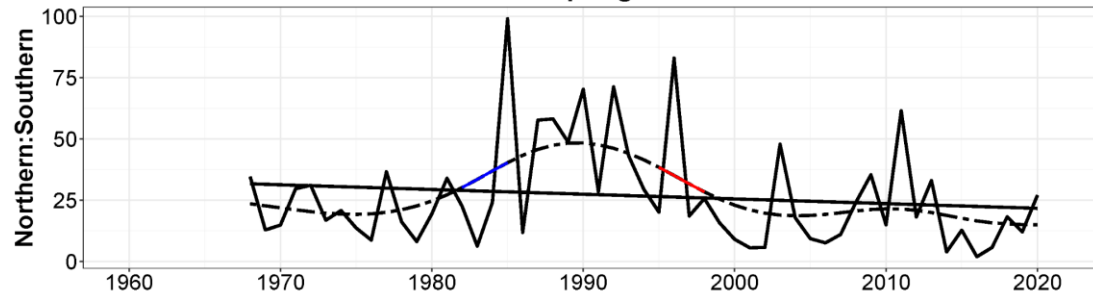


**Figure 31. Ratio northern to southern species biomass.** The dashed black line is the nonlinear GAM with periods of significant increasing trend in blue and decreasing trend in red. No significant linear trend was found.

### *Ratio of benthic to pelagic species*

Originally, we attempted to develop an indicator of reef-associated vs. non reef associated species. However, there were few reef-associated species that were consistently measured each year in the survey. For instance, snappers and groupers are only occasionally captured in a few years of the survey. We will continue to refine this indicator, but present here the ratio of benthic to pelagic species. Again, the biggest change in this indicator occurred in the 1960s likely as a result of intense fishing pressure on large benthic fishes (Fig. 32).

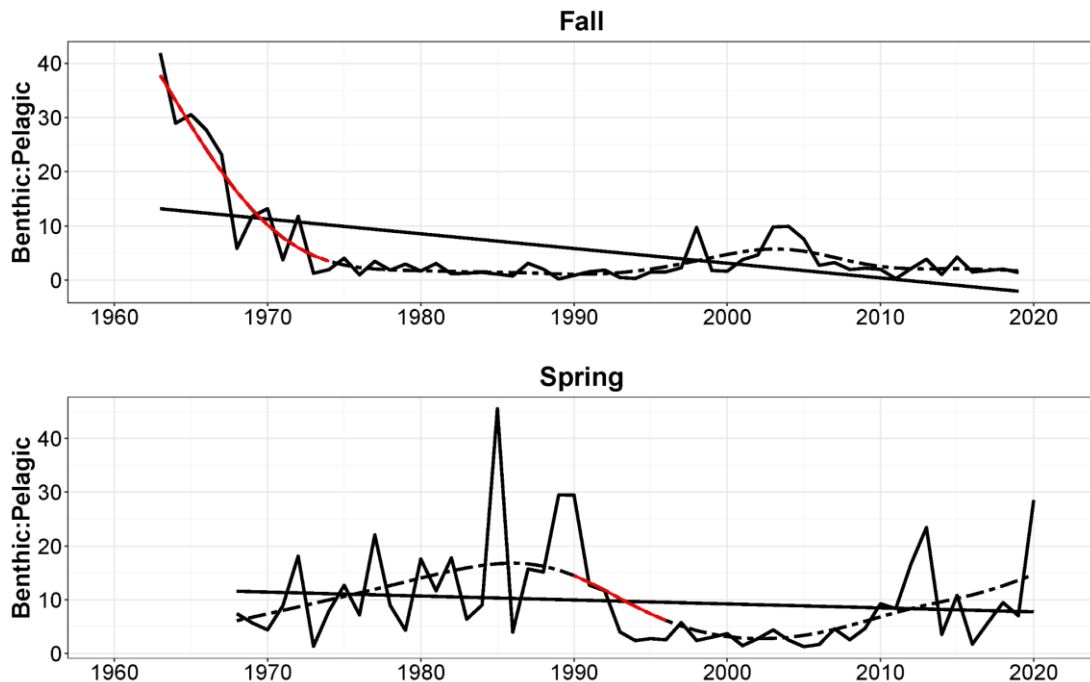


**Figure 32. Ratio of benthic to pelagic fish species.** There have been declines in the benthic species especially early in the time series. This is thought to be because of fishing pressure on large benthic fishes. The dashed black line is the nonlinear GAM with periods of significant increasing trend in blue and decreasing trend in red. No significant linear trend was found.

### *Fish species richness*

As waters warm, tropicalization of marine ecosystems is predicted. An indicator of such change is species richness, or the total number of species in the NYB in the NOAA bottom trawl survey. Species richness has increased steadily in the fall (Fig. 33). However, it has fluctuated quite a bit in the spring with a peak in 2011 followed by a recent decline.

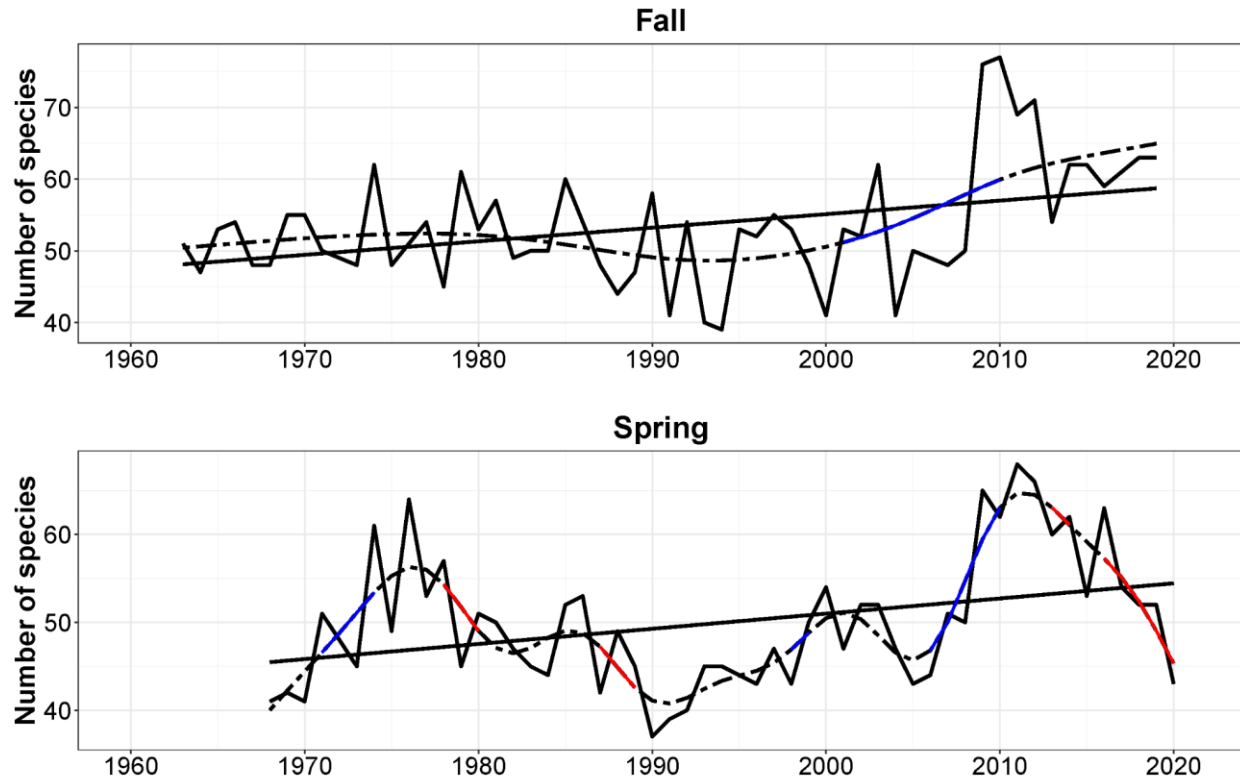


**Figure 33. Species richness (number of species) in the NOAA NEFSC bottom trawl survey.** The dashed black line is the nonlinear GAM with periods of significant increasing trend in blue and decreasing trend in red. No significant linear trend was found.

### *Average trophic level of fish community*

The average level of the fish community can be an indicator of overfishing of top predatory fishes or other changes in ecosystem structure and function. Trophic levels were taken from a food web model we are developing for the larger Mid-Atlantic Bight region. Trophic level in the fall seems to be steadily declining, but again fluctuating quite a bit more in the spring (Fig. 34).

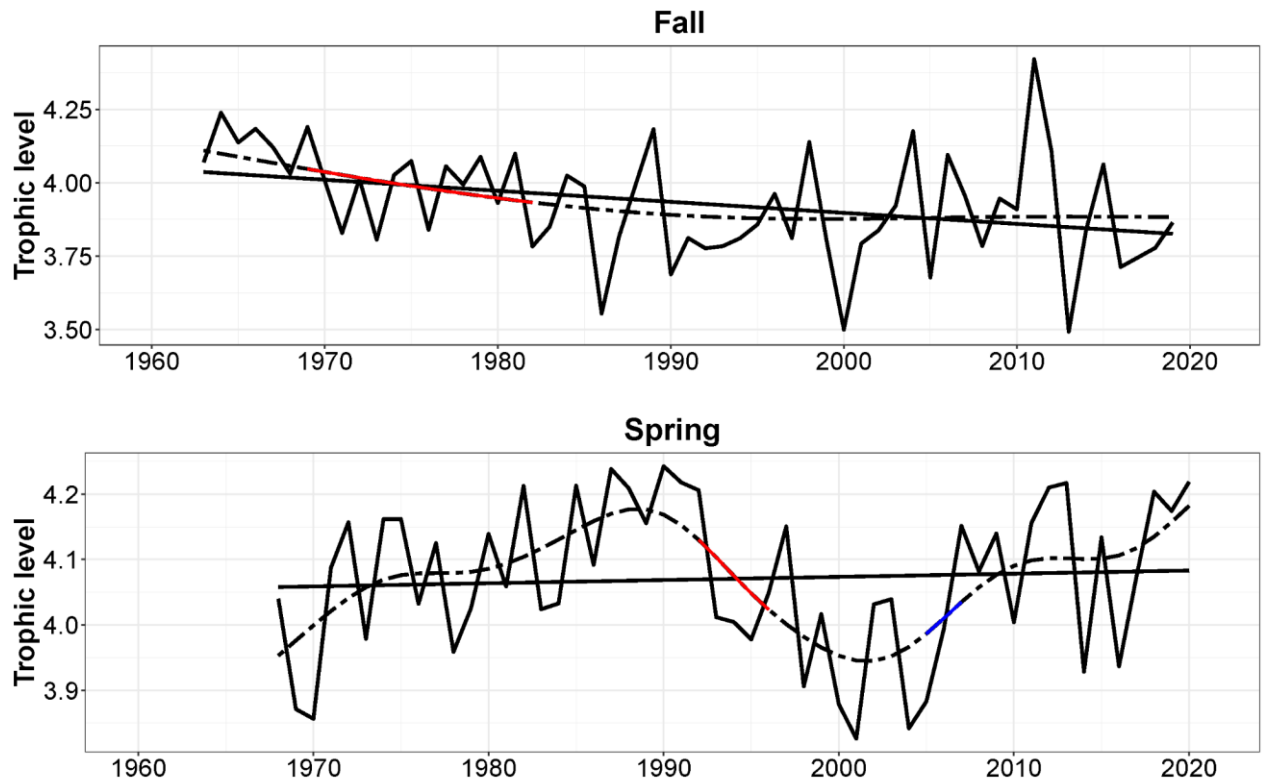


**Figure 34. Trophic level.** The dashed black line is the nonlinear GAM with periods of significant increasing trend in blue and decreasing trend in red. No significant linear trend was found.

### *Temperature preference of the fish community*

The temperature preference of the fish community as a whole is an indicator of warm water species becoming more abundant. To calculate this indicator, we estimated the biomass-weighted mean temperature of each fish species in the NOAA bottom trawl survey. Then we found the mean temperature of the community by taking the average temperature of each species and weighting by its biomass in each year. Thus, if warm water species are more abundant this indicator will increase. We see an increase in this indicator in both the Fall and Spring, but the timing of that change is different in each season (Fig. 35).

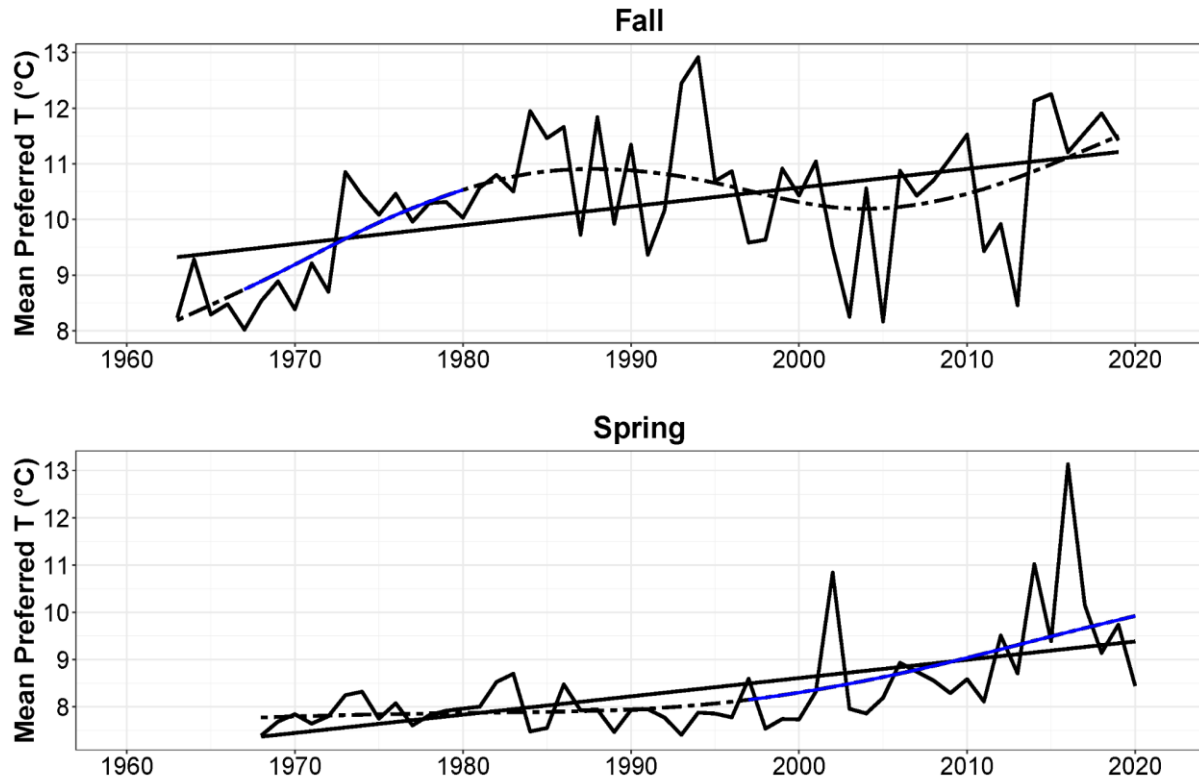


**Figure 35. Mean preferred temperature.** The dashed black line is the nonlinear GAM with periods of significant increasing trend in blue and decreasing trend in red. No significant linear trend was found.

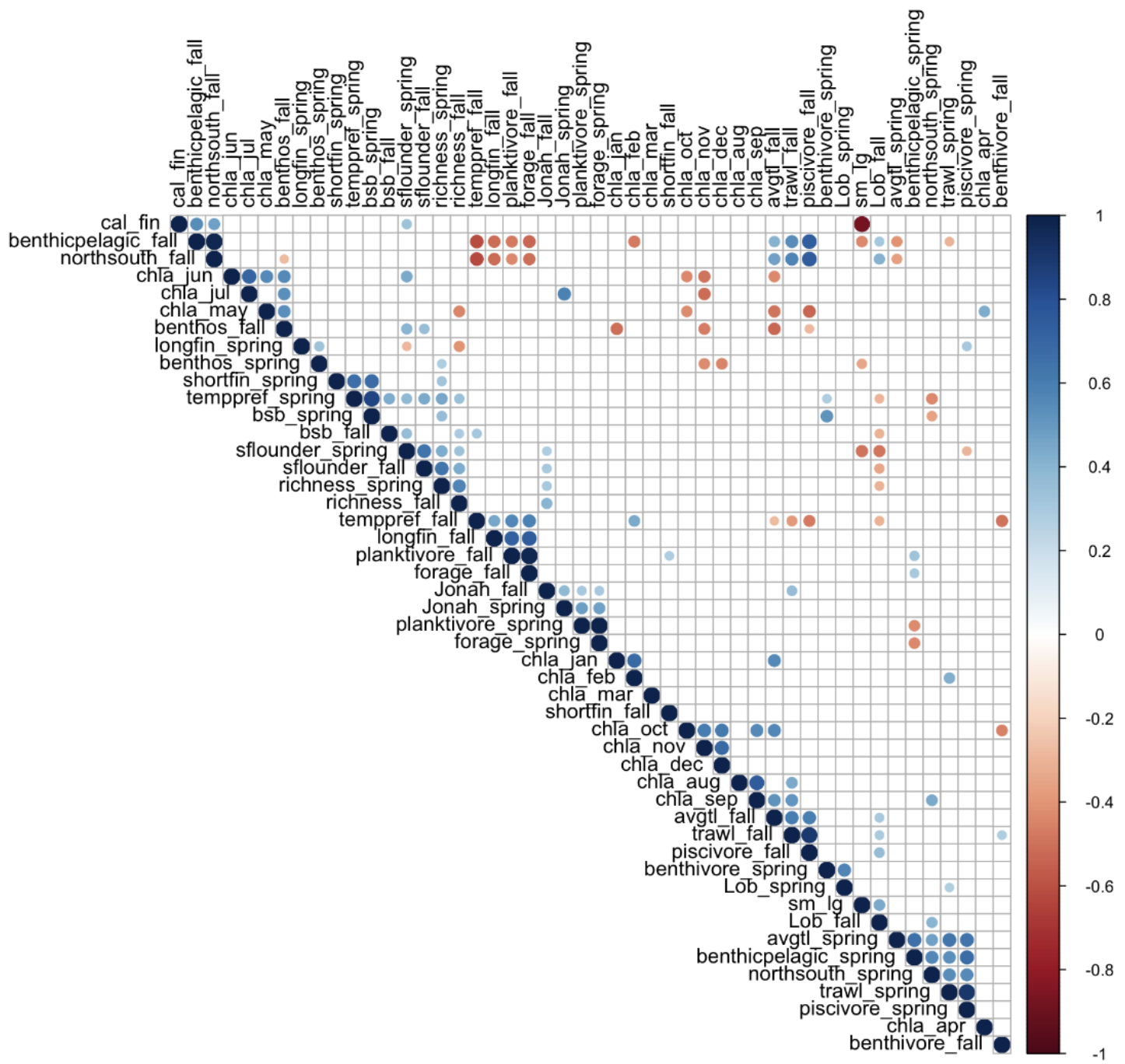


**Figure 36. Pairwise correlations amongst the marine community indicators.** Correlations between biological indicators with blank squares indicating non-significant ( $p>0.05$ ) correlations. Blue indicates a positive correlation while red indicates a negative correlation. The size of the circle as well as the color shading indicate the magnitude of the  $r$  value, with large values shown in deeper reds and blues and bigger circles.

### ***Summary for Marine Community Indicators***

The largest changes that we saw in the middle trophic levels occurred in the 1960s. At the start of the time series taken from the NOAA NEFSC bottom trawl survey there were increases in planktivores, decreases in piscivores, declines in benthic species, declines in the mean trophic level of the catch and the benthic:pelagic ratio. We did not see a clear trend over time in trawl biomass suggesting that as some trophic groups and species decline, other species increase in abundance to maintain total ecosystem productivity. These changes are all consistent with overfishing that occurred in the 1960s and 1970s that are well-documented (Fogarty and Muraski 1998). Since that time fishing pressure has decreased, but the ecosystem changes are now driven by climate change. Recently we have seen an increase in black sea bass and southern flounder (in the late 1990s-2000s) which likely increased as a result of good management and warming waters. We also see an increase in species richness in the fall and an increase in the mean temperature of the community. We did not see an increase in the ratio of northern to southern species. When examining the pairwise correlations between these indicators, it is interesting to see the strong negative correlation between benthic:pelagic species and the temperature preference of the community. Together, these time series illustrate that the change from more cold water to warm water species is not a phenomena limited to recent years. The change began in the 1960s when many large cold water species were overfished. Many of these species never recovered and the change to a more warm water assemblage has only continued over time.

## **5. Coastal Communities**

### ***Recreational harvest (total number all species)***

Care should be taken in interpreting this indicator as reporting changed over time, in particular there was a major change in 2000. However, these indicators include calibrations that correct for changes in the recreational harvest survey. In the future we will refine these indicators and investigate the proportion of recreational to commercial landings in NY.

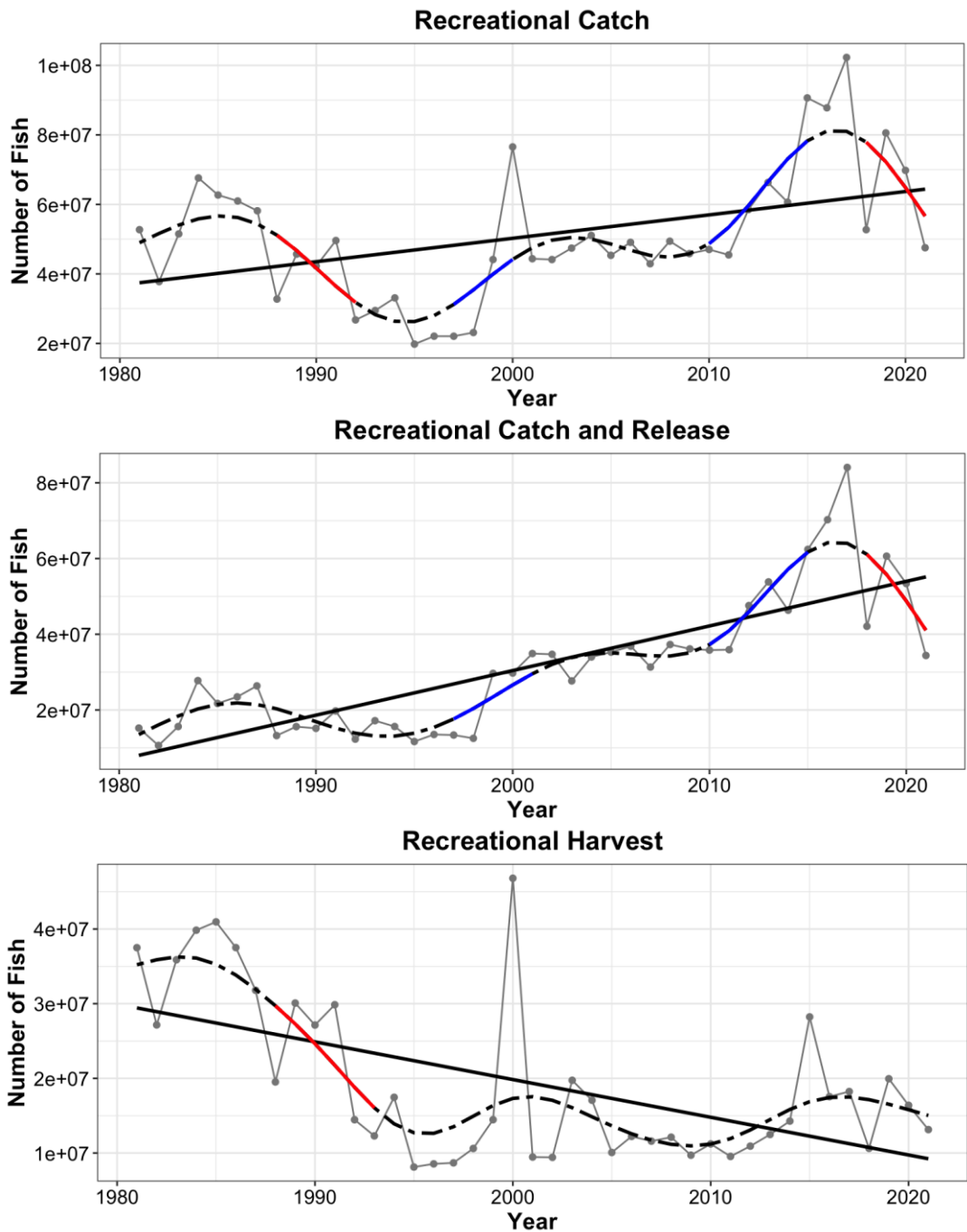


**Figure 37. Recreational Fishing.** (top) The total number of fish caught (harvested + catch and release) by recreational fishers. (middle) The number of fish caught and then released by recreational fishers. (bottom) The total recreational harvest in number of fish. Annual totals are in the dotted grey line, the statistically significant linear trend is shown by the solid black line and the nonlinear GAM in the dashed black line with periods of significant increasing trend in blue and significant decreasing trend in red.

### *Commercial fishing landings in NY*

#### **Commercial Harvest**

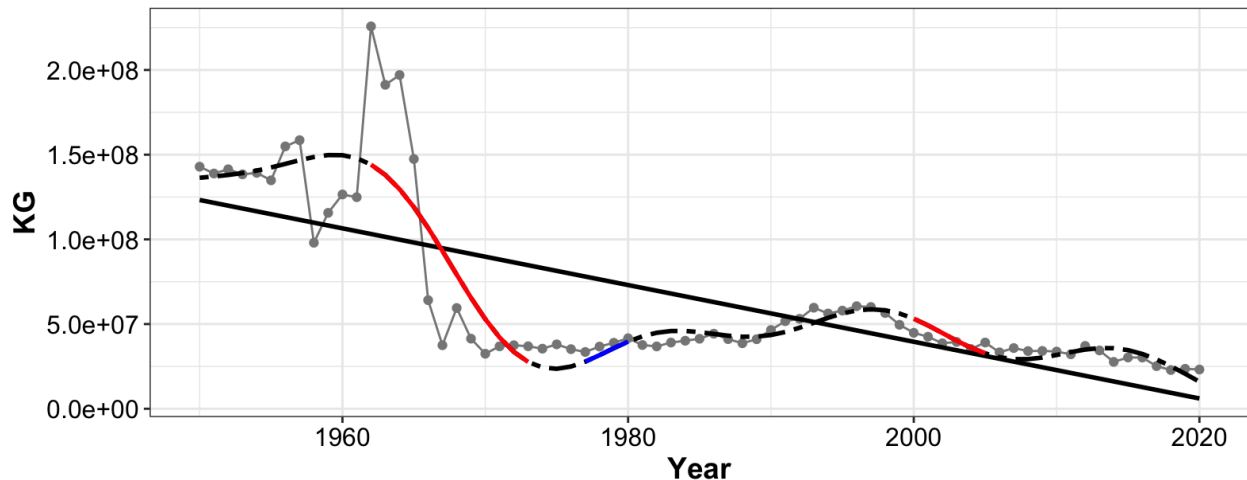


**Figure 38. Commercial fishing.** New York commercial harvest in pounds of fish. Annual totals are shown in dotted grey lines, the statistically significant linear trend in the solid black line and the nonlinear GAM in the dashed black line with periods of significant increase in blue and significant decrease in red.

### *Human population of Long Island*

This indicator has been updated to include the total population of Long Island (Nassau, Suffolk, Kings, and Queens counties) from the previous indicator report which only considered Nassau and Suffolk. The trend remains similar to the last report with a steady increase over time. However, a slight, but statistically significant decline is apparent in the last five years.

#### **Long Island Population**

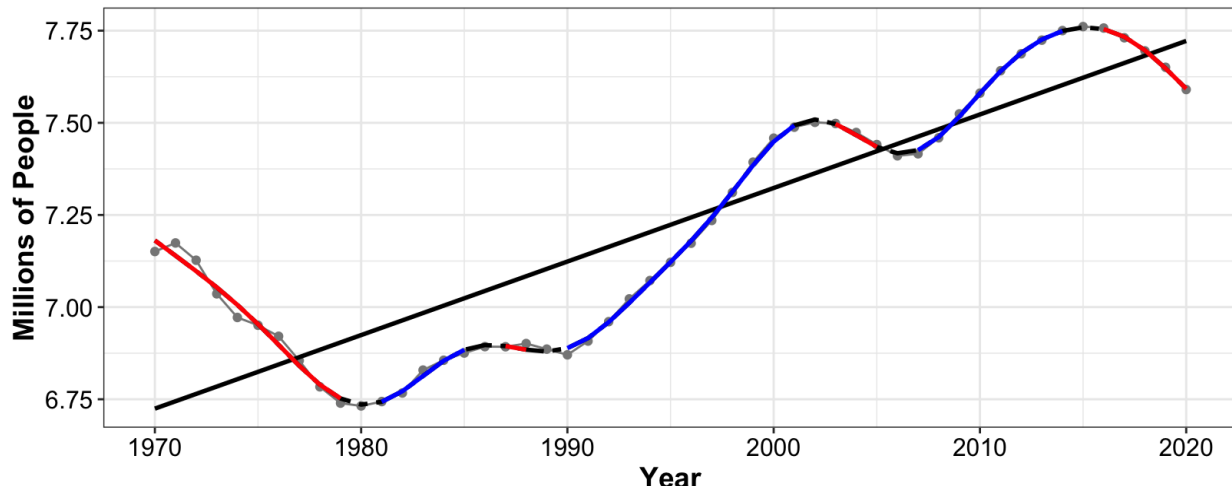


**Figure 39. Long Island population.** Human population of Suffolk, Nassau, Queens, and Kings counties. The grey dotted line shows yearly means. The solid black line shows the statistically significant ( $p < 0.05$ ) linear trend. The nonlinear GAM is shown in the black dashed line with periods of significant increasing trend in blue and significant decreasing trend in red.

## *Sea level risk for Long Island Communities*

The sea level rise risk map has not changed from the previous report, but we also included storm surge risk that was not included in the previous indicator report (Fig. 40). Colors indicate the risk relative to all other coastal communities in the US.

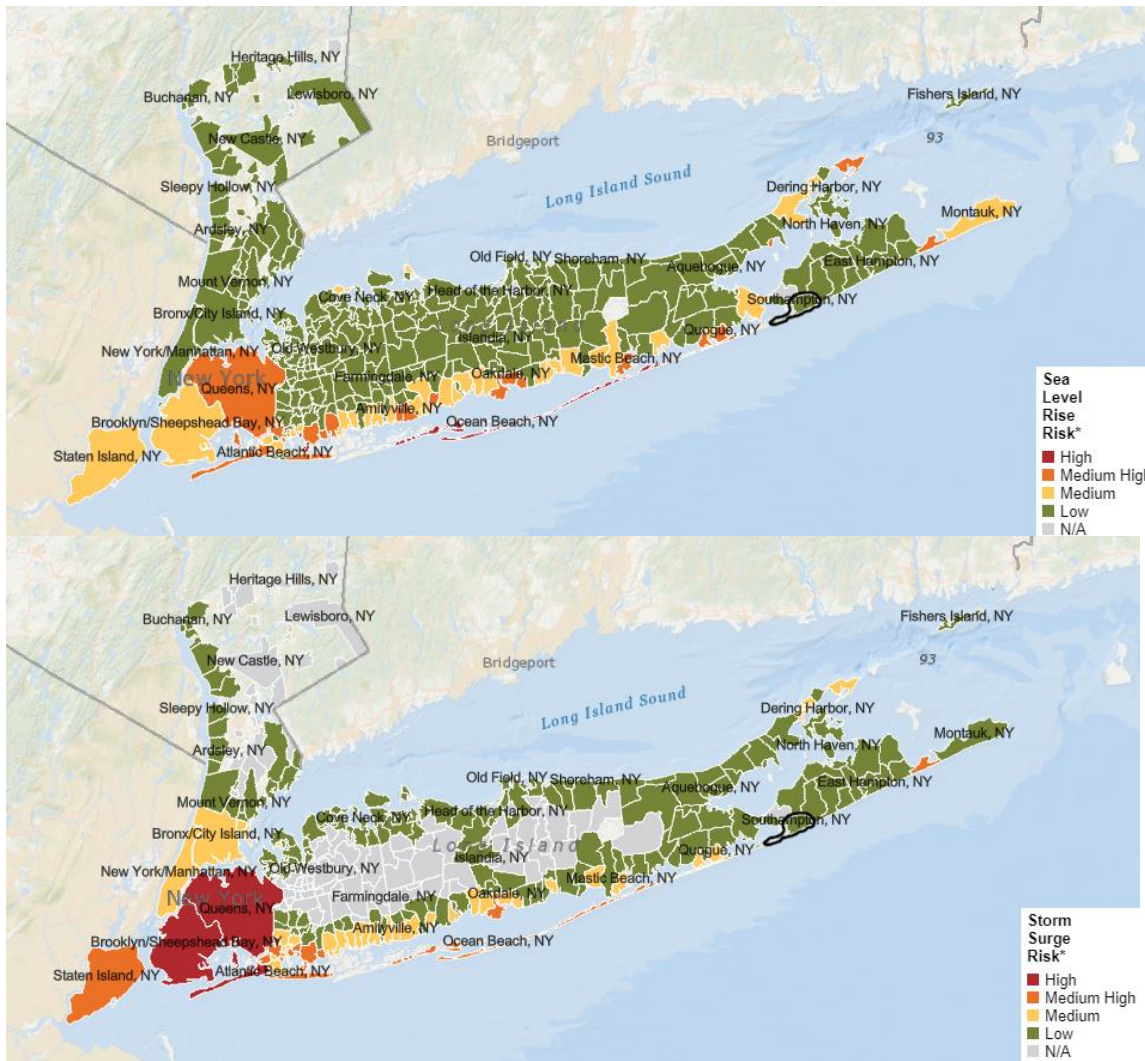


**Figure 40. Sea level risks.** Sea level rise risk (top) and storm surge risk (bottom) as estimated in 2018 by NOAA. Colors indicate the risk relative to other coastal communities in the United States.

## *Summary for Coastal Community Indicators*

Total recreational catch has been increasing in recent years, but the actual harvest has been decreasing over time indicating that although recreational effort has been increasing, most of these fish are released. Mortality can still be high depending on the season and species. Elasmobranchs and fishes without swim bladders tend to have low post release mortality, but swim bladdered fishes can have very high mortality especially when water temperature is high (summer and fall). Recreational fishing mortality can be a significant source of mortality for fish

stocks and this is an important indicator to monitor especially if the NYB is transitioning to an ecosystem that is more similar to the South Atlantic where recreational fishing is extremely important (Shertzer et al. 2018)

Communities near New York Harbor and on the south shore of Long Island have the highest relative sea level rise risk in NY, but are not rated among the highest risk across the country. The storm surge risk map for comparison illustrates the much higher risk to communities around NY Harbor for storm surge. These areas are at the highest risk for storm surge not only in NY, but in the entire country. Despite the sea level rise and storm surge risks posed to Long Island communities, Suffolk, Nassau, Kings, and Queens counties have seen an increase in population since the 1980s. These risks, unlikely to decrease with increased climate change, may put more people in danger if population trends continue to increase.

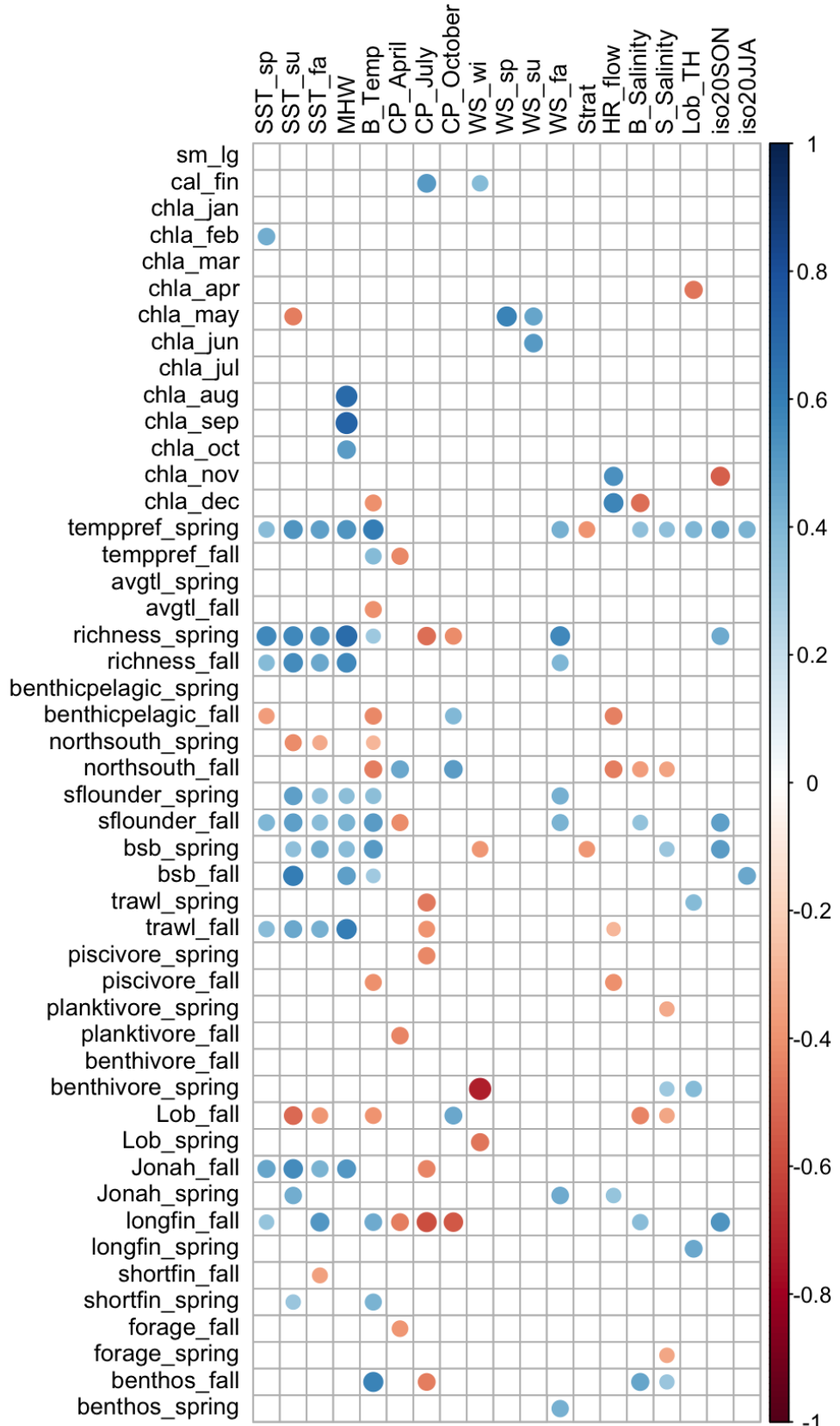


**Figure 41. Pairwise correlations of physical indicators and marine community indicators.**

Correlations between physical and biological indicators with blank squares indicating non-

significant ( $p>0.05$ ) correlations. Blue indicates a positive correlation while red indicates a negative correlation. The size of the circle as well as the color shading indicate the magnitude of the  $r$  value, with large values shown in deeper reds and blues and bigger circles.

## 6. Conclusions and Outlook for 2022

In agreement with the Indicator Report from 2020, we continue to see significant warming both at the surface and in bottom waters within the NYB. This subsurface warming is not yet sufficient to cause lethal thermal conditions for lobster communities at this time, though other marine communities such as bivalves may be threatened by the combination of warming temperatures, and relatively low aragonite saturation and dissolved oxygen during autumn. Further analysis of DO, pH, and aragonite saturation from subsequent years of Seawolf cruises will allow us to further constrain this seasonal cycle. Though warming may be harmful to some marine communities, for others it could be beneficial. Fig. 41 shows a positive correlation between both trawl biomass in the fall and species richness in the spring when compared to marine heatwave days. Surface chlorophyll in late summer to fall (August, September, and October) is also well correlated with marine heat wave days. This could indicate that even large increases in surface temperature could be beneficial to some organisms during certain seasons, although as noted previously this surface chlorophyll measurement does not have a one-to-one relation with primary production and should be interpreted with caution. Additionally, some specific species also show increased biomass with increased temperature such as black sea bass, summer flounder, and Jonah crab which are all well correlated with surface temperature and marine heatwave indicators.

Our initial analysis of cold pool volume indicates a potential for a shortened duration as October CP volume has plummeted in the last decade. This change could have an effect on longfin squid populations. These squid are an important commercial species for New York and their biomass is negatively correlated with our cold pool volume indicators. If the cold pool volume/duration is getting smaller/shorter, it could be beneficial to squid populations. The relationship between the cold pool and longfin squid will be investigated further in the coming year.

Our initial development of the cold pool volume indicator using GLORYS reanalysis data has many benefits, especially in terms of data coverage of our study area, but is not without drawbacks. Because this is reanalysis data we will always have a year or two lag between data availability and the year of the Indicator Report. In the coming year we aim to further incorporate the data from glider deployments. Glider data that overlaps spatially and temporally with the GLORYS reanalysis will help us not only to validate our cold pool volume indicator, but also to improve our understanding of cold pool development in real time. We will also continue to work on a cold pool duration indicator. As waters warm at the surface it is possible there may be an earlier onset of stratification, but bottom waters are warming as well so the cold pool core may not be as cold and dissolution might happen earlier in the autumn season.

The role of the Hudson River outflow into the NYB is also something we will continue to analyze. This river not only provides a source of lower salinity waters which could affect seasonal stratification, but is also a nutrient source and could be important for primary production. Hudson River outflow is well correlated with surface chlorophyll in late fall to winter (November to December; Fig. 41). We aim to use this correlation as a starting point to further investigate the role the Hudson plays in the physiochemical conditions of the NYB and in particular, the base of the food web.

## 7. References

- Fogarty, M. J., and S. A. Murawski. 1998. Large-scale disturbance and the structure of marine systems: fishery impacts on Georges Bank. *Ecological Applications* 8:S6-S22.
- Gangopadhyay, A., G. Gawarkiewicz, E. N. S. Silva, M. Monim, and J. Clark. 2019. An observed regime shift in the formation of warm core rings from the Gulf Stream. *Scientific Reports* 9:1-9.
- Henderson, M. E., K. E. Mills, A. C. Thomas, A. J. Pershing, and J. A. Nye. 2017. Effects of spring onset and summer duration on fish species distribution and biomass along the Northeast United States continental shelf. *Reviews in Fish Biology and Fisheries* 27:411-424.
- Joyce, T. M., and R. Zhang. 2010. On the path of the Gulf Stream and the Atlantic Meridional Overturning Circulation. *Journal of Climate* 23:3146-3154.
- Neto, A.G., J.A. Langan, and J.B. Palter. 2021. Changes in the Gulf Stream preceded rapid warming of the Northwest Atlantic Shelf. *Communications Earth & Environment* 2(74) <https://doi.org/10.1038/s43247-021-00143-5>
- Nye, J. A., T. M. Joyce, Y.-O. Kwon, and J. S. Link. 2011. Silver hake tracks changes in Northwest Atlantic circulation. *Nature Communications* 2:412.
- Pearce, J., and N. Balcom. 2005. The 1999 Long Island Sound lobster mortality event: Findings of the comprehensive research initiative. *Journal of Shellfish Research* 24:691-697.
- Quinn, B. K. 2017. Threshold temperatures for performance and survival of American lobster larvae: A review of current knowledge and implications to modeling impacts of climate change. *Fisheries Research* 186:383-396.
- Shertzer, K. W., E. H. Williams, J. K. Craig, E. E. Fitzpatrick, N. Klibansky, and K. I. Siegfried. 2019. Recreational sector is the dominant source of fishing mortality for oceanic fishes in

the Southeast United States Atlantic Ocean. *Fisheries Management and Ecology* **26**:621-629.

Stock, C. A., J. G. John, R. R. Rykaczewski, R. G. Asch, W. W. Cheung, J. P. Dunne, K. D. Friedland, V. W. Lam, J. L. Sarmiento, and R. A. Watson. 2017. Reconciling fisheries catch and ocean productivity. *Proceedings of the National Academy of Sciences* **114**:E1441-E1449.

Thomas, A. C., A. J. Pershing, K. D. Friedland, J. A. Nye, K. E. Mills, M. A. Alexander, N. R. Record, R. Weatherbee, and M. E. Henderson. 2017. Seasonal trends and phenology shifts in sea surface temperature on the North American northeastern continental shelf. *Elementa: Science of the Anthropocene* 5.

United States National Marine Fisheries Service, Northeast Fisheries Science Center (U.S.).  
2021. State of the Ecosystem 2021: Mid-Atlantic Revised  
DOI:<https://doi.org/10.25923/jd1w-dc26>

United States National Marine Fisheries Service, Northeast Fisheries Science Center (U.S.).  
2022. State of the Ecosystem 2022: Mid-Atlantic. *In Press*.

Vaquer-Sunyer, R., and C. M. Duarte. 2008. Thresholds of hypoxia for marine biodiversity. *Proceedings of the National Academy of Sciences* **105**:15452-15457.

## **New York Bight Indicator Report 2021 Appendix**

MOU #AM10560 NYS DEC & SUNY Stony Brook

Report contributors: Laura Gruenburg, Janet Nye, Lesley Thorne, Brandon Beltz, Tyler Menz, Baoshan Chen, Eleanor Heywood, Julia Stepanik, Joe Warren, Charlie Flagg

Contact Principal Investigator, Janet A. Nye with questions or comments  
janet.nye@stonybrook.edu

### **Part 2: Indicator Development**

#### **Summary**

This document provides additional detail and figures to show how some of the new indicators were developed. Information is also provided regarding indicators that are still under development including Humpback whale body condition and vessel density and speed.

#### **1. Physical and Chemical Indicators**

##### ***Fall transition date***

The fall transition date was calculated as in the Current Conditions of the Northeast U.S. Shelf Ecosystem: Spring 2021 Update produced by NOAA (<https://www.fisheries.noaa.gov/new-england-mid-atlantic/climate/current-conditions-northeast-us-shelf-ecosystem-spring-2021-update>). This thermal transition date was determined using SST data from Optimally Interpolated Sea Surface Temperature (OISST) v2.1 (<https://www.ncei.noaa.gov/products/optimum-interpolation-sst>) at 1/4° spatial and daily temporal resolution. For each latitude, longitude point within the NYB region a long term mean was determined by the climatological mean created from the first 30 years of data starting in 1982. This local mean was used as a reference at each lat lon location to delineate between the warm and cool portions of the year. A 5-day running mean was applied to each year of SST time series at each location to smooth out short lived anomalies that could affect the transition date. To determine the fall transition date, defined as the day of the year for each year where the SST shifts from the warm regime present in summer and autumn to cooler winter temperatures, we loop through days of the year 275 through 365 (roughly the beginning of October through the end of December) and determine at what day the SST drops below the local mean calculated in the first step. That day is recorded as the fall transition date for that particular year and location. Each lat lon point is represented by a grey dot in Figure 2. of Part 1.

##### ***Cold Pool Volume***

To calculate the volume of the cold pool a four dimensional dataset was needed which would provide temperature and salinity data by latitude, longitude and depth over time. We used the relatively fine scale GLORYS global ocean reanalysis product at  $1/12^{\circ}$  spatial, and monthly temporal resolution (Lellouche et al., 2021). The volume of the cold pool was defined by the temperature ( $10^{\circ}\text{C}$  or below) and salinity (34 PSU or below) criteria used in Chen et al. (2018) and Chen & Curchister (2020). Fig. 1 shows the volume of the cold pool based on these criteria within the NYB polygon for each year of the GLORYS data. The cold pool forms as the seasonal surface stratification is set up in the spring and dissolved with warming of the water column and increased vertical mixing in the fall (Houghton et al., 1982). Therefore, we looked at the cold pool volume during three different months - April, for the volume at cold pool onset; July, for the volume midway through the summer; October for the volume during the dissolution period.

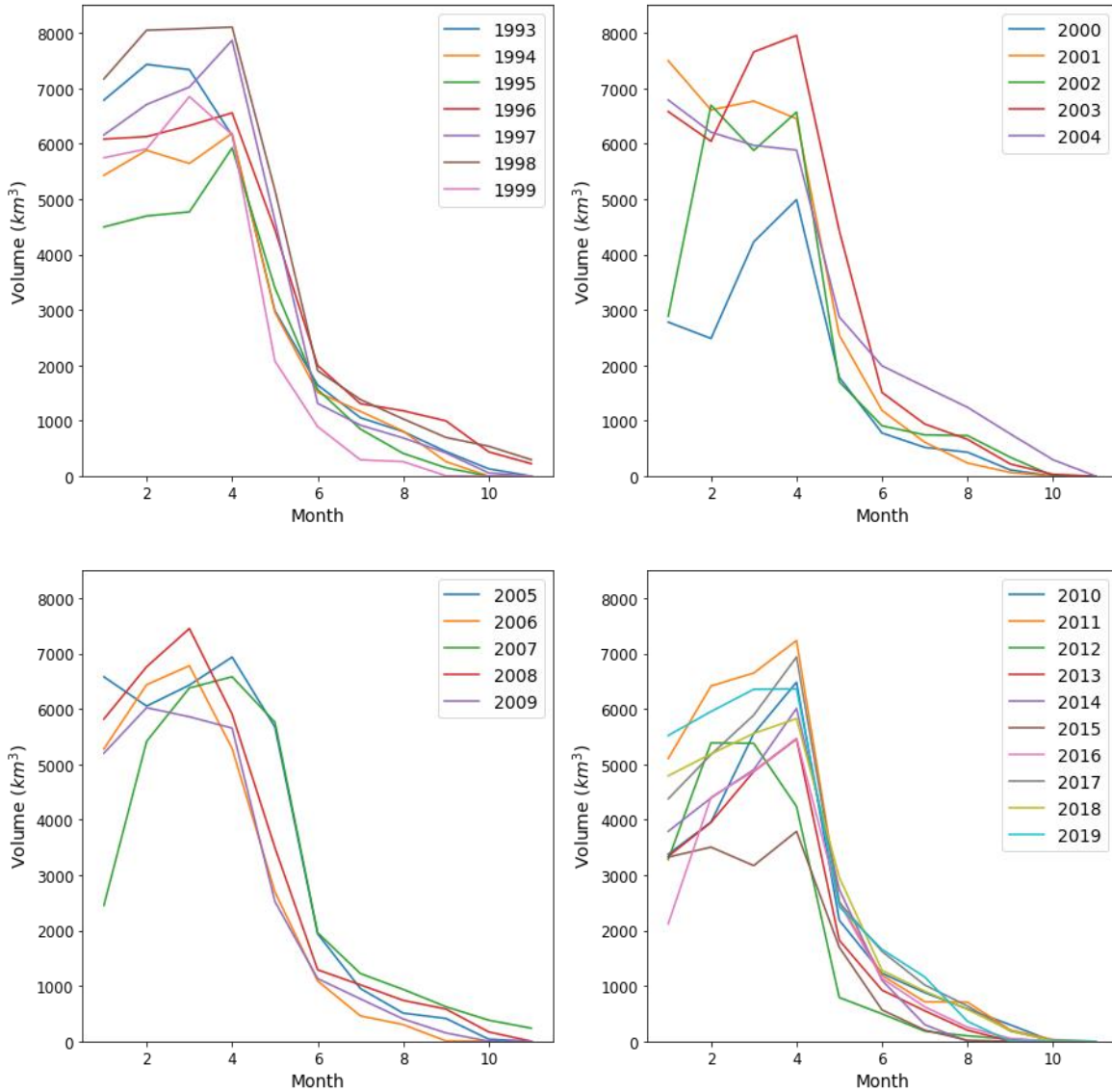


**Figure A1. Cold Pool Volume.** Volume of the cold pool within the NYB defined as waters at or below  $10^{\circ}\text{C}$  and 34 PSU using data from the GLORYS reanalysis. Clockwise from upper left are 1993 through 1999, 2000 through 2004, 2005 through 2009, and 2010 through 2019. The seasonality of the cold pool is evident with the onset of stratification and cold pool formation in

April, followed by warming of the water column throughout the summer and a dissolution of the cold pool in autumn.

### ***20°C surface isotherm***

Satellite data from OISST (Optimum Interpolation Sea Surface Temperature, <https://www.ncei.noaa.gov/products/optimum-interpolation-sst>) shows the 20°C surface isotherm present in the NYB region in the summer (Fig. 4; averaged June, July, August) and Autumn (Fig 5; averaged September, October, November) months. Over the course of the 1982 through 2020 observational time period the 20°C migrated north and, in some years, completely out of the NYB region. For this indicator we created a time series for summer showing the most eastward longitude of this isotherm for each year, and a time series for winter showing the most northward latitude of this isotherm. This may need to be adjusted in future reports as the summer 20°C surface isotherm has in many recent years completely exited the NYB leaving surface waters even warmer.

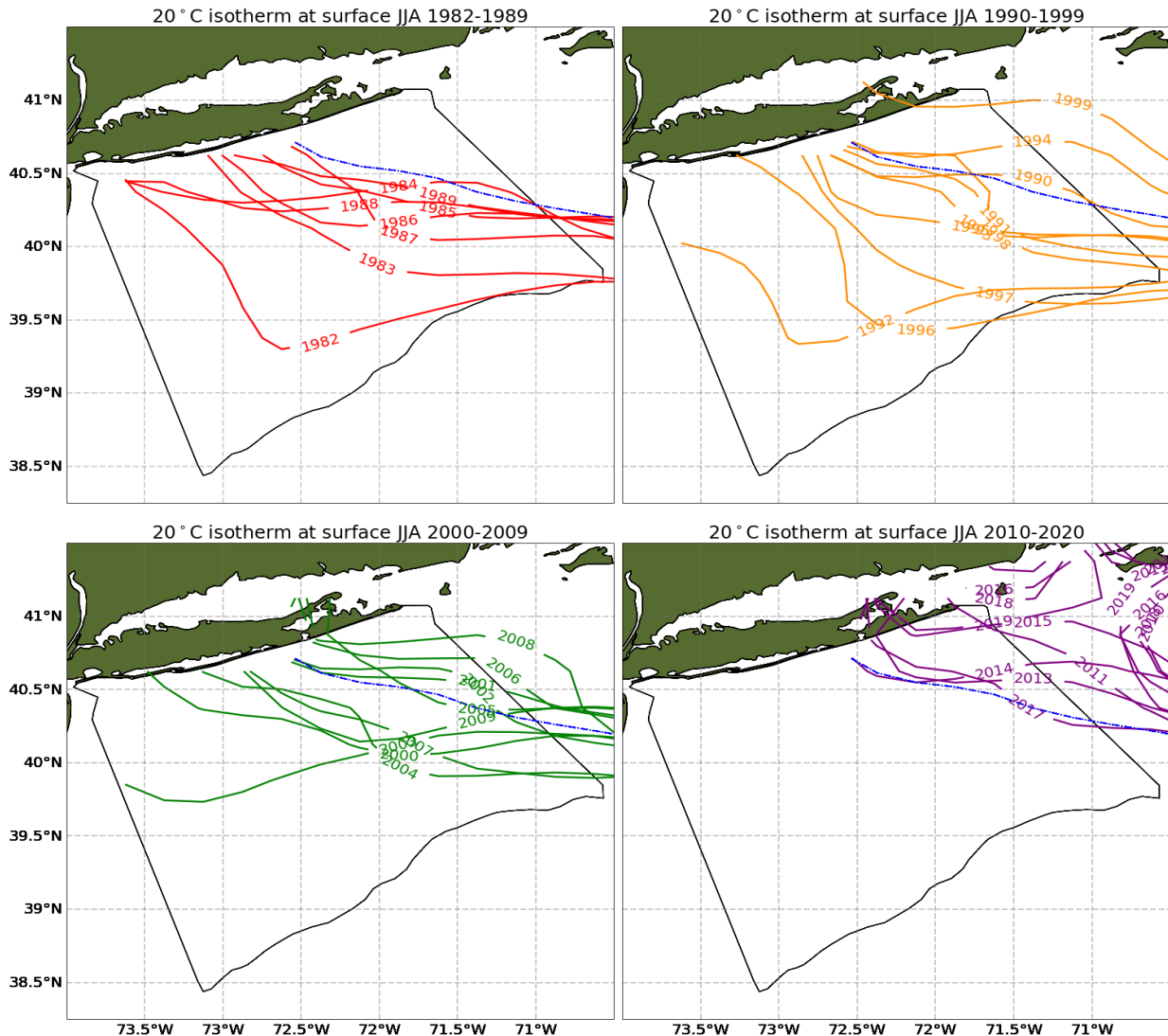


**Figure A2. Summer 20°C surface isotherm.** The surface 20°C isotherm from OISST data when averaged over summer months (JJA: June, July, August). The red lines show years 1982 through 1989, the orange lines 1990 through 1999, the green lines 2000 through 2009, and the purple lines 2010 through 2020. The dashed blue line shows the mean position of the 20°C surface isotherm across summers of the entire time series. The solid black line outlines the NYB polygon. This isotherm has been moving poleward over time, moving further northeastward from the 1980s to present.

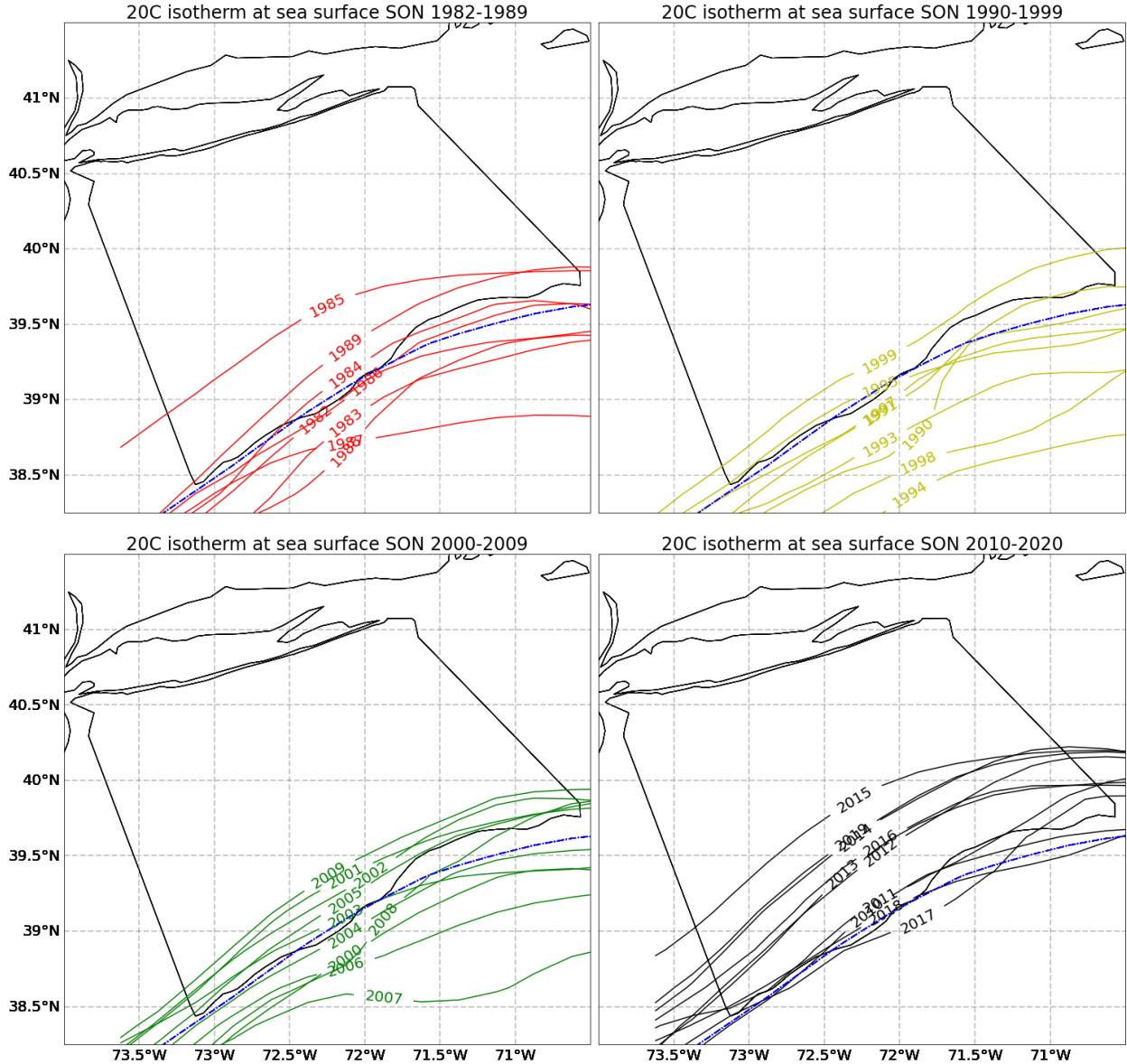


**Figure A3. Autumn 20°C surface isotherm.** The surface 20°C isotherm from OISST data when averaged over autumn months (SON: September, October, November). The red lines show years 1982 through 1989, the orange lines 1990 through 1999, the green lines 2000 through 2009, and the purple lines 2010 through 2020. The dashed blue line shows the mean position of the 20°C surface isotherm across autumns of the entire time series. The solid black line outlines the NYB polygon.

polygon. This isotherm has been moving poleward over time, moving further northward from the 1980s to present.

### ***Subsurface aragonite saturation state ( $\Omega_{Ar}$ ), corresponding pH and percent area***

Originally we were only asked to develop an indicator of surface carbonate chemistry parameters as a way to monitor ocean acidification. However, subsurface aragonite saturation state and pH are important to evaluate the stress on marine organisms especially calcifying organisms that are important to the NY economy. Aragonite is a more soluble form of calcium carbonate usually used in shell-forming organisms and is denoted by  $\Omega_{Ar}$ . Metabolic processes are greatly affected by even small changes in pH. We are developing these indicators of  $\Omega_{Ar}$  and pH by using field sampled discrete water samples and interpolation methods. With the analysis of water samples collected on cruises for dissolved inorganic carbon (DIC) and total alkalinity (TA) we can calculate aragonite saturation state ( $\Omega_{Ar}$ ) and pH. Once these data were obtained we first defined some ecologically-relevant thresholds for  $\Omega_A$ . Aragonite values less than 1 are undersaturated with respect to aragonite and most shelled organisms cannot form shell at this level. However, even  $\Omega_{Ar} > 1$  could be stressful to marine organisms and it becomes more energetically expensive for organisms to form shell as  $\Omega_{Ar}$  approaches 1. The more energy an organism has to use to form shell the less energy it can use for growth, reproduction and survival. Thus, we preliminarily use  $\Omega_{Ar}=1.5$  as the threshold to evaluate potentially stressful waters for shellfish and also to calculate a pH indicator.  $\Omega_{Ar}$  and pH usually have different distribution patterns, i.e. low  $\Omega_{Ar}$  water might correspond to either high pH or low pH waters, we use pH data corresponding to the low  $\Omega_{Ar}$  water to develop the indicator of subsurface pH. In addition, the percent area of low subsurface  $\Omega_{Ar}$  is developed to estimate the expansion of acidic bottom water.

The water column chemistry data is contoured for each transect in each year (e.g. Figure A4). A contour line is drawn to delineate the threshold of interest, in this case  $\Omega_{Ar} < 1.5$ . The indicator is then the average of  $\Omega_{Ar}$  values across all transects sampled for each cruise. Since sampling can be inconsistent, we also report its standard deviation, minimum, and maximum values.

Correspondingly, we do the same calculation for observed pH values to give us numbers of how low the pH are (Table A1, using 2019 data as a case study). As for the percent area of subsurface low  $\Omega_{Ar}$  water, we first estimate the area of the transect spanning from the most inshore station to the most offshore station and account for the bottom topography. Second, we plot the contour of pre-defined threshold for  $\Omega_{Ar}$  and estimate its area. Finally, the percent area of low  $\Omega_{Ar}$  water is calculated by dividing the area of low  $\Omega_{Ar}$  water by the transect area (Table A2). It should be noted that due to Covid and bad weather, we were unable to cover all transects in every season. Spring and fall were less sampled while summer was most sampled. Particularly in the fall cruise, we only covered transects 1 and 2 which are located in the easternmost portion of the New York Bight. In this case, it is difficult to accurately evaluate the aragonite saturation state and its corresponding percent area on the unsampled transects in which  $\Omega_{Ar}$  might be lower and percent area might be larger. It highlights the need to have a consistent spatial coverage in future field

research. Although we can only illustrate this approach with one year of data, we will be able to look at annual trends in the upcoming years as more water samples are processed.

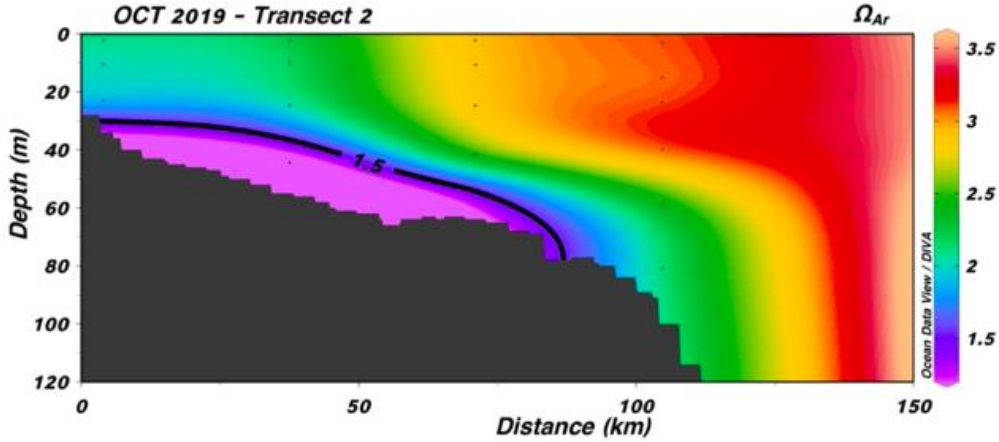


**Figure A4. Aragonite saturation state transect 2 October 2019.** An example of how the aragonite saturation state indicator was developed. The faint black dots indicate CTD casts that are then contoured in ODV software. Using a threshold of  $\Omega_{\text{Ar}}=1.5$  the area under that contour is estimated.

Table A1. Summary of seasonal subsurface aragonite saturation states ( $\Omega_{\text{Ar}}$ ) and corresponding pH in areas with  $\Omega_{\text{Ar}}<1.5$  in 2019, with average $\pm$ standard deviation and ranges presented.

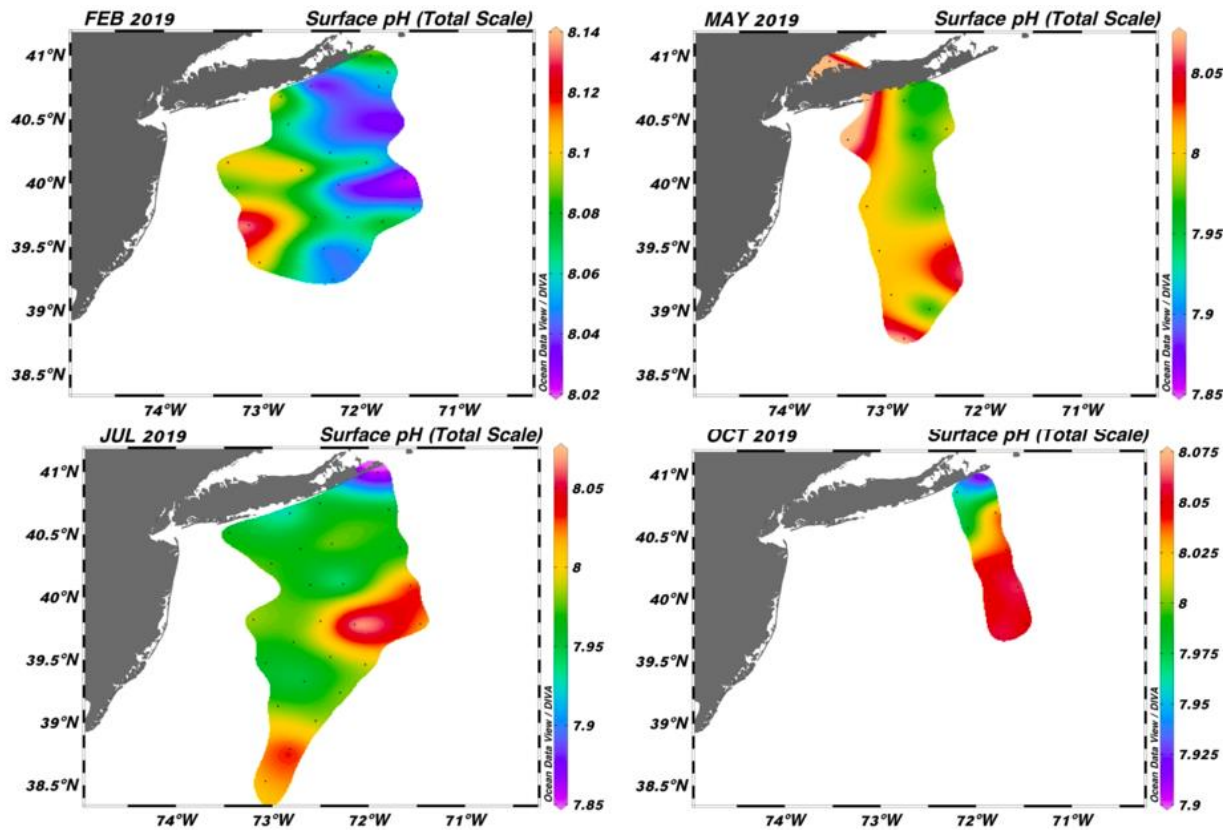
	$\Omega_{\text{Ar}}$		pH		Number of samples
	Average $\pm$ s.d.	Range	Average $\pm$ s.d.	Range	
Winter (NYOS1902)	1.47 $\pm$ 0.03	1.41-1.49	8.038 $\pm$ 0.053	7.977-8.085	5
Spring (NYOS1905)	1.36 $\pm$ 0.07	1.27-1.49	7.956 $\pm$ 0.024	7.922-7.990	11
Summer (NYOS1907)	1.32 $\pm$ 0.10	1.18-1.49	7.914 $\pm$ 0.043	7.780-7.972	35
Fall (NYOS1910)	1.20 $\pm$ 0.27	0.90-1.45	7.809 $\pm$ 0.082	7.710-7.877	4

Table A2. Seasonal variation in percent area of  $\Omega_{\text{Ar}}<1.5$  water on transect 1 and 6 in 2019.

	Winter (NYOS1902)	Spring (NYOS1905)	Summer (NUOS1907)	Fall (NYOS1910)
Transect 1	1.7%	N/A	28.1%	6.8%
Transect 6	0.0%	13.0%	14.6%*	N/A

\*We were unable to sample every depth on transect 6 in 2019, thus the percent area is substantially underestimated.

Similarly, we have developed the indicators of surface aragonite saturation state ( $\Omega_{\text{Ar}}$ ) and pH to monitor ocean acidification. Surface water is defined as the water in the surface mixed layer, usually corresponding to the top 5 m water and the surface water samples we collected in the NYOS cruises. Surface contours for  $\Omega_{\text{Ar}}$  and pH are first plotted to study the spatial variation and seasonal variation (Figure A5, using pH as an example). Then we report the average, standard deviation, minimum, and maximum values for all of the surface samples collected for every season (Figure 8 in Part 1). Due to the inconsistent transects covered resulting from covid and bad weather, our ability to conduct a seasonal variation analysis for a consistent area is limited. However, the standard deviation, minimum, and maximum values provide context and uncertainty in these estimates. Currently 2019 is used as a case study, but as we collect more samples we will be able to look at annual trends in the upcoming years.



**Figure A5. 2019 surface pH.** Distribution of surface pH for four cruises in 2019.

### **Bottom Dissolved Oxygen**

The data used to examine bottom dissolved oxygen (mg/L) comes from CTD casts during offshore cruises on the R/V Seawolf. We used the last depth at each station or the depth closest to

100 m to define the bottom for this analysis. We did not use any depths greater than 100 m as these would be stations beyond the shelf break where the depths are so deep that the CTD did not come anywhere near the bottom. We are interested in examining both the bottom dissolved oxygen (DO) and a value for DO that overlaps with areas of low aragonite saturation and pH. Microbial respiration tends to decrease available oxygen while simultaneously producing carbon dioxide and low pH. Preliminary analysis has shown that areas where we are observing low DO do not always correspond perfectly to area as low aragonite saturation and pH, but in those places where they do co-occur are likely to be stressful to marine organisms.

We are employing the same method described for aragonite saturation and pH to determine the percentage area of DO within each transect that overlaps with the low aragonite saturation areas. We also performed a sensitivity test where we calculated the percentage area covered for various DO levels at each transect. An example of the values obtained from one sensitivity analysis can be seen in Table A3.

Table A3: Results of the dissolved oxygen sensitivity analysis from transect 6 on the May 2019 cruise.

DO threshold (mg/L)	DO Area (km <sup>2</sup> )	Percentage of area below threshold
6.3	0.0	0
6.4	0.3	2.4
6.8	0.8	6.5
7.4	1.8	14.6
7.8	2.8	22.8
8.0	3.5	28.5
8.2	5.5	44.7

## 2. Marine Community

### *Humpback whale body condition*

As large, long-lived animals that feed at a high trophic level, marine mammals serve as effective indicators of the health of marine ecosystems (Bossart et al. 2011, Hazen et al. 2019). The body condition of individual animals provides a metric of energy reserves relative to body size, and is often used to assess individual and population status and health. Baleen whales show pronounced seasonal migrations, and forage intensively to increase their energy reserves while on high latitude foraging grounds. Studying the body condition of baleen whales on their foraging grounds reflects the accumulation of energy reserves in that region, and can thus provide an indicator of resource availability. Assessing changes in baleen whale body condition through time can provide key information on changes to resource availability, while comparing body condition across foraging areas can provide information on the relative availability of resources in a particular area.

We are developing an indicator of the body condition of humpback whales in the NYB by integrating Unmanned Aerial Vehicle (UAV) measurements with a scalable three-dimensional (3D) model to estimate body volume, which provides a holistic means of assessing body volume

(Hirtle et al. in review). There are two indicators that we are developing from this monitoring effort: 1. A temporal indicator that will assess changes to the body condition of humpback whales foraging in New York waters through time (i.e., quantify interannual variability); and 2. A spatial indicator that will compare the body condition of humpback whales foraging in New York waters with those in different foraging areas across the North Atlantic. Together these objectives will allow us to understand the importance of the NYB resources on body condition in humpback whales. Condition indices for upper trophic levels are an excellent indicator of ecosystem health of the New York Bight because they integrate across multiple trophic levels.

### ***Odontocete Strandings data***

To provide an analogous indicator for marine mammals to the fish and zooplankton indicators that convey the relative abundance of northern vs. southern species we are examining strandings data. Cetaceans are key predators in marine ecosystems and serve as important sentinels of changes to ocean conditions and food webs (Aguirre and Tabor 2004, Moore 2008, Hazen et al. 2019). Records of cetacean stranding events provide important data for understanding changes to cetacean distribution through time (MacLeod et al. 2005, Evans and Hammond 2004, Pyenson 2011, Thorne and Nye 2021). Using the framework of MacLeod (2009), we are assessing how the occurrence of odontocete species in different climatic categories has changed through time in New York State. Preliminary analyses suggest that the species composition of odontocetes has shown considerable changes over the past 25 years in association with warming waters.

## **3. Coastal Communities**

### ***Vessel Density and Speed***

Human civilization has long relied on ocean spaces for transporting a wide range of information and goods. While historically these human industries were more coastally distributed, in recent history they have expanded further into pelagic ecosystems as technology has made some of the most remote parts of the ocean accessible. Termed the “Blue Acceleration”, human activities in marine regions have also increased substantially in frequency and intensity over the last 50 years (Jouffray et al. 2020). The New York Bight is home to the United States’ third largest commercial shipping port, a rich culture of commercial and recreational fishing, and eight active lease areas for offshore wind energy development, and is thus strongly impacted by anthropogenic pressure. Inherent to anthropogenic activity in ocean spaces is the use of vessels of all sizes for transportation of materials and people. Thus, monitoring and summarizing spatio-temporal trends in vessel traffic can serve as an indicator for anthropogenic pressure on ecosystems and specific taxonomic groups within New York waters. For example, vessel strike is a major conservation issue facing populations of large whales, and thus understanding trends in vessel traffic in New York is key to understanding risk of vessel strike for these protected species (Stepanuk et al. 2021).

Automatic Identification System (AIS) is an automated ship tracking system that has been used increasingly in recent decades to provide information on vessel traffic in coastal waters. In the US, AIS transmits a vessel’s unique identifier along with positional data (including speed) every

2-3 minutes to a network of land and satellite-based receivers. While the satellite data is propriety, the U.S. government operates the Nationwide Automatic Identification System (NAIS), a series of land-based VHF receivers designed to increase Maritime Domain Awareness (BOEM). These receivers reliably detect all positional data from any participating vessels within approximately 40-50 miles of land. These data are free to the public and provide hundreds of millions of point locations from tens of thousands of vessels across 6 usage sectors (tanker, tug/tow, fishing, passenger, recreation, and research/industry).

We are developing an indicator of vessel traffic in the New York Bight through time using AIS data. The time frame of our analysis is influenced by regulatory changes governing the required use of AIS transmitters by different vessel types and lengths and by recent mandates from insurance policies requiring some user groups (e.g. smaller sport fishing vessels) to carry AIS transmitters. These changes complicate our ability to make direct comparisons between recent and historical time periods. Preliminary analyses of vessel density demonstrate that AIS usership is relatively stable from 2015 onward and we are thus focusing our analysis on publicly available data beginning in year 2015. Vessel density in 10km X 10km grid cells is being assessed for each month in years 2015-2020. These grid cells will then be assessed spatially and temporally, and will be summed for the New York Bight region across relevant time scales to look at vessel density across different vessel categories to assess changes in ocean use in the NYB over time.

#### 4. References

- Aguirre, A.A. and Tabor, G.M., 2004. Introduction: marine vertebrates as sentinels of marine ecosystem health. *EcoHealth* 1(3):236-238.
- Bureau of Ocean Energy Management (BOEM) and National Oceanic and Atmospheric Administration (NOAA). [MarineCadastre.gov](#). {Nationwide Automatic Identification System 2015-2020}. Retrieved {2021} from [marinecadastre.gov/data](#)
- Bossart, G.D., 2011. Marine mammals as sentinel species for oceans and human health. *Veterinary pathology* 48(3):676-690.
- Chen, Z., E. Chuchister, R. Chant, and D. Kang. 2018. Seasonal variability of the Cold Pool over the Mid-Atlantic Bight Continental Shelf. *Journal of Geophysical Research Oceans* 123(11):8203-8226. <https://doi.org/10.1029/2018JC014148>
- Chen, Z. and E.N. Curchister. 2020. Interannual variability of the Mid-Atlantic Bight Cool Pool. *Journal of Geophysical Research Oceans* 125(8). <https://doi.org/10.1029/2020JC016445>
- Evans, P.G.H., and P. S. Hammond. 2004. Monitoring cetaceans in European waters. *Mammal Review* 34(1):131-156.
- Hazen, E.L., B. Abrahms, S. Brodie, G. Carroll, M.G. Jacox, M.S. Savoca, K.L. Scales, W.J. Sydeman, and S.J. Bograd. 2019. Marine top predators as climate and ecosystem sentinels. *Frontiers in Ecology and the Environment* 17(10): 565-574.

- Hirtle, N.O., J.E.F. Stepanuk, E.I. Heywood, F. Christiansen, and L.H. Thorne. *In review.*  
Integrating 3D models with morphometric measurements to improve volumetric estimates  
in large mammals. *Methods in Ecology and Evolution*
- Houghton, R. W., R. Schlitz, R.C. Beardsley, B. Butman, and J.L. Chamberlin. 1982. The Middle  
Atlantic Bight Cold Pool: evolution of the temperature structure during Summer  
1979. *Journal of Physical Oceanography* 12(10):1019-1029.
- Jouffray, J-B., R.Biasiak, A.V. Norström, H. Österblom, and M. Nyström. 2020. The blue  
acceleration: the trajectory of human expansion into the ocean. *One Earth* 2 1: 43–54.  
<https://doi.org/10.1016/j.oneear.2019.12.016>.
- Lellouche, J-M., E. Greiner, R. Bourdallé-Badie, G. Garric, A. Melet, M. Drévillon, C. Bricaud,  
M. Hamon, O. Le Galloudec, C. Regnier, T. Candela, C-E. Testut, F. Gasparin, G.  
Ruggiero, M. Benkirane, Y. Drillet, and P-Y. Le Traon. 2021. The Copernicus Global  
1/12° Oceanic and Sea Ice GLORYS12 Reanalysis. *Frontiers in Earth Science* 9  
DOI=10.3389/feart.2021.698876.
- MacLeod, C.D., S.M. Bannon, G.J. Pierce, C. Schweder, J.A. Learmonth, J.S. Herman, and R.J.  
Reid. 2005. Climate change and the cetacean community of north-west Scotland.  
*Biological Conservation* 124:477–483.
- MacLeod, C.D., 2009. Global climate change, range changes and potential implications for the  
conservation of marine cetaceans: a review and synthesis. *Endangered Species Research*  
7(2):125-136.
- Moore, S.E., 2008. Marine mammals as ecosystem sentinels. *Journal of Mammalogy* 89(3):534-  
540.
- Pyenson, N.D. 2011. The high fidelity of the cetacean stranding record: insights into measuring  
diversity by integrating taphonomy and macroecology. *Proceedings of the Royal Society B*  
278(1724):3608-3616.
- Stepanuk, J.E.F., E.I. Heywood, J.F. Lopez, R.A. DiGiovanni Jr, and L.H. Thorne. 2021. Age-  
specific behavior and habitat use in humpback whales: implications for vessel strike.  
*Marine Ecology Progress Series* 663: 209–22. <https://doi.org/10.3354/meps13638>.
- Thorne, L. H., and J. A. Nye. 2021. Trait-mediated shifts and climate velocity decouple an  
endothermic marine predator and its ectothermic prey. *Scientific reports* 11(1):1-14.